HHS Public Access

Author manuscript

Neurobiol Dis. Author manuscript; available in PMC 2020 December 01.

Published in final edited form as:

Neurobiol Dis. 2019 December ; 132: 104535. doi:10.1016/j.nbd.2019.104535.

Differential toxicity of ataxin-3 isoforms in *Drosophila* models of Spinocerebellar Ataxia Type 3

Sean L. Johnson[a,1], **Jessica R. Blount**[a,1], **Kozeta Libohova**[a], **Bedri Ranxhi**[a], **Henry L. Paulson**[b], **Wei-Ling Tsou**[a,*], **Sokol V. Todi**[a,c,*]

[a]Department of Pharmacology, Wayne State University School of Medicine, Detroit, MI, USA

[b]Department of Neurology, University of Michigan Medical School, Ann Arbor, MI, USA

[c]Department of Neurology, Wayne State University School of Medicine, Detroit, MI, USA

Abstract

The most commonly inherited dominant ataxia, Spinocerebellar Ataxia Type 3 (SCA3), is caused by a CAG repeat expansion that encodes an abnormally long polyglutamine (polyQ) repeat in the disease protein ataxin-3, a deubiquitinase. Two major full-length isoforms of ataxin-3 exist, both of which contain the same N-terminal portion and polyQ repeat, but differ in their C-termini; one (denoted here as isoform 1) contains a motif that binds ataxin-3's substrate, ubiquitin, whereas the other (denoted here as isoform 2) has a hydrophobic tail. Most SCA3 studies have focused on isoform 1, the predominant version in mammalian brain, yet both isoforms are present in brain and a better understanding of their relative pathogenicity *in vivo* is needed. We took advantage of the fruit fly, *Drosophila melanogaster* to model SCA3 and to examine the toxicity of each ataxin-3 isoform. Our assays reveal isoform 1 to be markedly more toxic than isoform 2 in all fly tissues. Reduced toxicity from isoform 2 is due to much lower protein levels as a result of its expedited degradation. Additional studies indicate that isoform 1 is more aggregation-prone than isoform 2 and that the C-terminus of isoform 2 is critical for its enhanced proteasomal degradation.

*Corresponding authors at: Wayne State University School of Medicine, Department of Pharmacology, 540 E. Canfield, Scott Hall, Detroit, MI 48201, USA. wtsou@wayne.edu (W.-L. Tsou), stodi@wayne.edu (S.V. Todi).

[1]Equal contribution.

Authors' contributions

Designed study: SLJ, JRB, W-LT, SVT.
Conducted experiments and collected data: SLJ, JRB, KL, BR, W-LT, SVT.
Interpreted results and prepared figures: SLJ, JRB, KL, BR, HLP, W-LT, SVT.
Contributed to manuscript preparation: SLJ, JRB, KL, BR, W-LT, SVT.
Finalized manuscript: SLJ, JRB, HLP, W-LT, SVT.
All authors read, edited and approved the final version of the manuscript.

Declarations of Competing Interests

The authors declare that they have no competing interests.

Ethics and approval consent to participate

Not applicable.

Consent for publication

Not applicable.

Availability of data and materials

All pertinent results are included in main figures and in supplemental materials. All tools and materials generated for this work will be made available upon request to the corresponding authors.

Appendix A. Supplementary data

Supplementary data to this article can be found online at https://doi.org/10.1016/j.nbd.2019.104535.

According to our results, although both full-length, pathogenic ataxin-3 isoforms are toxic, isoform 1 is likely the primary contributor to SCA3 due to its presence at higher levels. Isoform 2, as a result of rapid degradation that is dictated by its tail, is unlikely to be a key player in this disease. Our findings provide new insight into the biology of this ataxia and the cellular processing of the underlying disease protein.

Keywords

Ataxia; *Drosophila*; Isoform; Neurodegeneration; Polyglutamine; Proteasome

1. Introduction

Several ataxias are caused by specific genetic mutations. Among these is the most common ataxia in the world, Spinocerebellar Ataxia Type 3 (SCA3), also known as Machado-Joseph Disease (Costa Mdo and Paulson, 2012; Matos et al., 2019). An age-related disorder, SCA3 is a member of the family of polyglutamine (polyQ)-dependent diseases alongside other SCAs (1, 2, 6, 7 and 17), Huntington's Disease, Kennedy's Disease, and Dentatorubropallidoluysian Atrophy. PolyQ diseases are caused by abnormal lengthening of a CAG triplet repeat in the respective genes, which translates into an expanded polyQ stretch in the encoded proteins. Expanded polyQ in each of these disease proteins causes misfolding and the formation of aggregates, neuronal dysfunction and death (Buijsen et al., 2019; La Spada and Taylor, 2003; Lieberman et al., 2019; Paulson et al., 2017; Todi et al., 2007a; Zoghbi and Orr, 2000, 2009).

SCA3 is a progressive ataxia accompanied by dystonia, dysarthria, spasticity, rigidity, ophthalmoparesis, dysarthria, dysphagia and neuropathy. Pathology includes degeneration of cerebellar pathways and nuclei, pontine and dentate nuclei, substantia nigra, globus pallidus, cranial motor nerve nuclei and anterior horn cells. SCA3 is caused by abnormal triplet CAG repeat expansion in the gene *ATXN3* that is normally 12–42 repeats in length, but is expanded to ~60–84 in patients (Costa Mdo and Paulson, 2012; Matos et al., 2019). Expansion occurs in the protein ataxin-3, a deubiquitinase (DUB) implicated in quality control (Costa Mdo and Paulson, 2012; Matos et al., 2019). Although ataxin-3 is widely expressed, degeneration is constrained to specific areas of the brain. Histopathologically, the SCA3 protein is found in macroaggregates/inclusions in the cytoplasm and in the nucleus (Costa Mdo and Paulson, 2012; Matos et al., 2019; Paulson et al., 1997a).

Extensive work by various laboratories provided insight into enzymatic properties and potential functions of the SCA3 protein. As a DUB, ataxin-3 binds and cleaves ubiquitin chains of a specific length and type (Costa Mdo and Paulson, 2012; Matos et al., 2019; Weishaupl et al., 2019; Winborn et al., 2008). Ataxin-3 may have different types of substrates, depending on the needs of the cell, and might even function as a monitor of ubiquitin homeostasis. In cultured mammalian cells and in the fruit fly, *Drosophila melanogaster*, ataxin-3 is important during proteotoxic stress (Tsou et al., 2013, 2015b; Warrick et al., 2005). *In vivo*, according to different *atxn3* knockout lines, this protein

appears dispensable (Costa Mdo and Paulson, 2012; Matos et al., 2011; Schmitt et al., 2007; Switonski et al., 2011; Zeng et al., 2013).

PolyQ expansions in ataxin-3 most likely cause disease though a toxic gain-of-function, although the precise nature of the dominant toxic properties remains elusive. What is clear is the fact that nuclear ataxin-3 is markedly more toxic than its cytoplasmic portion, and that aggregation of disease-causing ataxin-3 precedes and correlates with cellular dysfunction and disease (Bichelmeier et al., 2007; Ristic et al., 2018; Schmidt et al., 1998; Costa Mdo and Paulson, 2012; Matos et al., 2019). Preventing aggregation of the SCA3 protein is beneficial to cells, tissues and organisms harboring polyQ-expanded ataxin-3 (Costa Mdo and Paulson, 2012; Matos et al., 2011, 2019; Ristic et al., 2018; Sutton et al., 2017; Tsou et al., 2015a). Still, our understanding of SCA3 biology remains incomplete.

Towards understanding SCA3, we reasoned that it will be beneficial to comprehend the toxicity of the products of its causative gene, *ATXN3*. Two major isoforms of ataxin-3 arise by alternative splicing of *ATXN3* mRNA (Harris et al., 2010). The original ataxin-3 variant isolated from SCA3 human brain (Kawaguchi et al., 1994), which we refer to as isoform 2 in this work, encodes a version containing 2 Ubiquitin-interacting motifs (UIMs), the polyQ repeat and a C-terminal stretch of hydrophobic amino acids (Fig. 1A). Subsequent studies identified another variant, referred to as isoform 1, that encodes a third UIM at its C-terminus (Goto et al., 1997) (Fig. 1A). Isoform 1 of ataxin-3 is the predominant form in the mammalian brain; isoform 2 is also present in this organ, but at lower levels than isoform 1 (Harris et al., 2010). Due to a lack of reagents that can readily and reliably distinguish these isoforms, it is unclear whether specific forms are enriched in certain types of cells or tissues in the normal and diseased brain.

Isoform 2 appears to aggregate more rapidly *in vitro* and in cultured mammalian cells. In cultured cells, isoform 2 protein is also less stable than isoform 1 (Harris et al., 2010). These informative observations notwithstanding, a comprehensive understanding of the relative toxicity and pathogenic contribution of each isoform is presently lacking *in vivo*. Here, we investigated the toxicity of each isoform of pathogenic ataxin-3 by generating novel, isogenic *Drosophila melanogaster* transgenics that encode ataxin-3 protein with a polyQ of 80, within human disease range. We observe that isoform 1 of pathogenic ataxin-3 is much more toxic than isoform 2, as a result of higher turnover and lower steady state levels of the latter variant. We also find that both isoforms are degraded by the proteasome and autophagy. Collectively, our results yield new information on the pathogenicity of the ataxin-3 isoforms *in vivo*, present new genetic tools to further assess toxic products of the *ATXN3* gene, and expand overall understanding of SCA3 biology.

2. Materials and methods

2.1. Constructs and plasmids

We used the company Genscript (genscript.com) to synthesize human ataxin-3 cDNA with a CAGCAA repeat that encodes 80Q. The nucleotide sequences used for isoforms 1 and 2 were based on ataxin-3 sequences described in prior publications (Harris et al., 2010; Sutton et al., 2017; Todi et al., 2009; Winborn et al., 2008), but with a CAGCAA repeat instead of a

pure CAG tract to circumvent the possibility of repeat-associated non-ATG (RAN) translation and mRNA toxicity (Figura et al., 2015; Green et al., 2016; Li et al., 2008; Marti, 2016; Shieh and Bonini, 2011; Sobczak et al., 2003; Sobczak and Krzyzosiak, 2005; Stochmanski et al., 2012). Constructs were subcloned into pcDNA3.1 for mammalian expression and pWalium-10.moe for fly line generation by using *Eco*RI (5′) and *Xba*I (3′) restriction digest sites. A Kozak sequence, shown in Fig. 1D, was added 5′ onto the ataxin-3 cDNA sequence for fly expression and the endogenous Kozak of pcDNA3.1 was utilized for expression in mammalian cells. An HA tag-encoding sequence was added immediately after the last nucleotide of the ataxin-3 sequence, as shown in Fig. 1A. Each construct was sequence-verified before utilization for its intended purposes. Genscript was also used to synthesize the ataxin-3 constructs in Fig. 9 and subclone them into pcDNA3.1 through EcoRI (5′) and XbaI (3′) digestion/ligation.

2.2. Drosophila stocks and new transgenic lines

All fly stocks and crosses were maintained at 25 °C and ~60% humidity in diurnal incubators with 12 h light/dark cycles. Common stocks were from the Bloomington *Drosophila* Stock Center (BDSC). New transgenic lines were generated through phiC31-dependent integration of transgenes into the attP2 site of the fly's third chromosome, as we have done in the past (Ristic et al., 2018; Sutton et al., 2017; Tsou et al., 2015b, 2016). New lines generated were verified to ensure insertion at the correct site (PCR-based assays), in the correct orientation (PCR-based assays) and sequence-verified for transgene nucleotide sequence. The lines generated for the work in this manuscript all contain a CAGCAA repeat to encode the expanded polyQ of ataxin-3. The only exception is the fly line that we denote here as "weaker expressing isoform 1", which contains a pure CAG repeat and was described in our prior publications (Costa et al., 2016; Ristic et al., 2018; Sutton et al., 2017). This latter transgene is also inserted on chromosome 3 of *Drosophila*, and on the same genetic background as the other two isoform lines.

Fly lines used here are as follows: GMR-Gal4 (#8121) and the isogenic host strain attP2 (#36303) were from BDSC. RNAi lines were from BDSC and the Vienna *Drosophila* RNAi Center (VDRC): RNAi to Atg7 (BDSC34369 (#1), BDSC27707 (#2)); Atg8a (BDSC34340 (#1), BDSC28989 (#2)); Atg12 (BDSC27552 (#1), BDSC34675 (#2)); Rpn1 (BDSC34348 (#1), VDRC25549 (#2), VDRC103939 (#3)); prosα5 (BDSC34786); prosβ2 (BDSC67363). The following lines were gifts: sqh-Gal4 driver (Dr. Daniel P. Kiehart, Duke University), elav-Gal4-GS driver (Dr. R. J. Wessells, Wayne State University), elav-Gal4 driver and repo-Gal4 driver (Dr. Daniel F. Eberl, University of Iowa). Unless otherwise stated in the figure legends and text, all flies were heterozygous for driver and transgene.

2.3. Longevity and motility assays

Adult flies were collected after eclosion from their pupal cases and were aged at 25 °C on conventional cornmeal fly media or RU486-containing media, as noted in the text, figures and figure legends. Flies were switched to vials with fresh food every 2–3 days. Each vial was examined for death each day, until all flies were dead. Motility was tested weekly through negative geotaxis: approximately 10 flies per vial were forced to the bottom of the vial by gentle tapping on the bench. The total number of adult flies that reached the top of

the vial at 5, 15 and 30 s was recorded and expressed as a percentage of total flies. Adults were transferred to fresh vials 1 h before assessment, and every 2–3 days for the duration of the experiment; their longevity was monitored daily.

2.4. Mammalian cells and assays

HeLa and HEK-293 T cells were purchased from ATCC and cultured in DMEM supplemented with 10% FBS and 5% Penicillin-Streptomycin, under conventional conditions. The day before transfection, cells were seeded in 12-well plates. Cells were transfected using Lipofectamine LTX (Invitrogen) per manufacturer's directions. Twenty-four hours after transfection, cells were treated as indicated in figure legends with cycloheximide (100 μg/ml; A. G. Scientific), and/or MG132 (20 μM; A. G. Scientific) or chloroquine (100 μM, A. G. Scientific). Cells were harvested in hot SDS lysis buffer for western blotting (see below).

2.5. Western blotting

Five whole flies, five pupae or ten dissected adult fly heads per group were homogenized in boiling lysis buffer (50 mM Tris pH 6.8, 2% SDS, 10% glycerol, 100 mM dithiothreitol), sonicated, boiled for 10 min, and centrifuged at 13,300 × g at room temperature for 10 min. The same lysis buffer and procedures were used for extraction of protein from mammalian cells. Samples were electrophoresed on 4–20% gradient gels (BioRad). Western blots were developed using the charge-coupled device-equipped VersaDoc 5000MP system (BioRad) or PXi 4 (Syngene). Blots were quantified using Quantity One software (BioRad) or GeneSys (Syngene). Direct blue staining was used for loading: PVDF membranes were submerged for 5 min in 0.008% Direct Blue 71 (Sigma-Aldrich) in 40% ethanol and 10% acetic acid. PVDF membranes were then rinsed briefly in 40% ethanol and 10% acetic acid solvent, then ultrapure water, air dried, and imaged.

2.6. Differential centrifugation

Ten whole flies per group were lysed in 200 μl of NETN buffer (50 mM Tris, pH 7.5, 150 mM NaCl, 0.5% Nonidet P-40), supplemented with protease inhibitor cocktail (PI, SigmaFast Protease Inhibitor Cocktail Tablets; Sigma-Aldrich), sonicated at 50% for 15 s and centrifuged at 20,000 ×*g* for 30 min at 4 ℃. The supernatant was transferred to a new microfuge tube and quantified by the BCA assay (Thermo Scientific). The pellet was resuspended in 200 μl of PBS + 1% SDS, vortexed, and boiled. Thirty micrograms of the supernatant fraction and 7 μl of the pellet fraction were supplemented with 6× SDS, boiled, and loaded onto SDS-PAGE gels gels for western blotting.

2.7. Filter-trap assay

Three whole flies per group were lysed in 200 μl of NETN+PI. Lysates were diluted with 200 μl PBS containing 0.5% SDS, sonicated at 50% for 15 s, and centrifuged at 4000 ×*g* for 1 min at room temperature. One hundred microliters of supernatant were diluted with 400 μl PBS. Seventy microliters of sample were filtered through a 0.45 μm nitrocellulose membrane (Schleicher & Schuell) using a Bio-Dot apparatus (BioRad) and analyzed by Western blotting.

2.8. Nuclear/cytoplasmic extraction

Fractionation was conducted using the ReadyPrep Protein Extraction Kit (Cytoplasmic/Nuclear; BioRad) to separate cytoplasmic and nuclear proteins. Five whole, adult flies were lysed in cytoplasmic extraction buffer (BioRad). Nuclei were resuspended in Protein Solubilization Buffer (BioRad). Samples were analyzed by western blotting, where, proportionally, 3× nuclear fraction was loaded compared to cytoplasmic fraction to eliminate need for over-exposure. Note: through this particular kit and protocol, banding and smearing of ataxin-3 protein signal can vary among blots, likely as a result of buffers as well as different kit and antibody batches; this is highlighted through two different examples in Fig. 2C and Supplemental fig. 2. For quantification purposes, we quantified ataxin-3 signal from the entire lane, including main band and smear above it.

2.9. Antibodies

Anti-Ataxin-3 (mouse monoclonal 1H9, 1:500–1000; Millipore) (rabbit polyclonal, 1:15,000; Paulson et al., 1997b), anti-GAPDH (mouse monoclonal MAB374, 1:500; Millipore), anti-tubulin (mouse monoclonal T5168, 1:10,000; Sigma-Aldrich), anti-HA (rabbit monoclonal, 1:500–1000; Cell Signaling Technology), anti-lamin (mouse monoclonal ADL84.12–5, 1:1000; Developmental Studies Hybridoma Bank), peroxidase conjugated secondary antibodies (goat anti-mouse and goat anti-rabbit, 1:10,000; Jackson Immunoresearch).

2.10. qRT-PCR

Total RNA was extracted from whole, adult flies using TRIzol (Life Technologies). Extracted RNA was treated with TURBO DNAse (Ambion). Reverse transcription was carried out using the high capacity cDNA reverse transcription kit (ABI). mRNA levels were quantified using the StepOne Real-Time PCR system with Fast SYBR Green Master Mix (ABI). Primers used:

ATXN3 F: 5′ -GAATGGCAGAAGGAGGAGTTACTA- 3′;

ATXN3 R: 5′ -GACCCGTCAAGAGAGAATTCAAGT- 3′;

rp49 F: 5′ -AGATCGTGAAGAAGCGCACCAAG- 3′;

rp49 R: 5′ -CACCAGGAACTTCTTGAATCCGG- 3′.

2.11. Statistics

Student's *t*-tests, ANOVA with post-hoc assays and log-rank tests were conducted for statistical comparisons, as indicated in the figure legends. Software utilized was GraphPad Prism and Apple Numbers. Graphs were generated in Apple Numbers.

3. Results

3.1. New Drosophila lines to investigate SCA3

As summarized in Fig. 1A, earlier studies (Bettencourt et al., 2010; Goto et al., 1997; Harris et al., 2010; Ichikawa et al., 2001; Kawaguchi et al., 1994; Paulson et al., 1997a; Schmidt et al., 1998; Weishaupl et al., 2019) established that two major, full-length isoforms arise from alternative splicing of *ATXN3* mRNA; a polymorphism in what we term isoform 2 in this study also gives rise to a slightly shorter variant that is denoted by the arrowhead in Fig. 1A. The ataxin-3 variants are identical, except for their respective C-termini. As noted earlier, both of these forms are present in mammalian brain, but isoform 1 is predominant (Harris et al., 2010). Here, we focus on the pathogenic property of the two full-length isoforms, depicted in the lower part of Fig. 1A. We generated constructs that encode either human ataxin-3 isoform with an expanded polyQ (80), which is within patient range. The transgenes are used through the Gal4-UAS binary expression system in the fly (Brand and Perrimon, 1993), which enables expression in a tissue- and time-dependent manner (Ristic et al., 2018; Sutton et al., 2017; Tsou et al., 2015a,b; 2016).

We designed the polyQ of ataxin-3 to be encoded by CAGCAA doublet repeats. Expanded *ATXN3* may lead to neuronal toxicity not only through the ataxin-3 protein, but also *via* mRNA toxicity as a result of a long, homogenous CAG trinucleotide repeat (Li et al., 2008). Moreover, in addition to encoding polyQ, the expanded CAG repeat of *ATXN3* could lead to repeat-associated non-AUG (RAN) translation of non-polyQ homopolymers, as observed in other CAG expansion repeat disorders (Banez-Coronel et al., 2015; Zu et al., 2011, 2018). For the purposes of this study, we sought to focus on toxicity from the polyQ-expanded ataxin-3 protein. Therefore, to avoid the potential confound of RAN translation and mRNA toxicity, the polyQ of ataxin-3 is encoded by alternating CAGCAA repeats. This approach precludes the production of proteins in alternative frames and eliminates potential *ATXN3* mRNA toxicity (Figura et al., 2015; Green et al., 2016; Li et al., 2008; Marti, 2016; Shieh and Bonini, 2011; Sobczak et al., 2003; Sobczak and Krzyzosiak, 2005; Stochmanski et al., 2012). The polyQ-reading frame has an HA epitope tag at its C-terminus and we capped the other two sense reading alternatives with in-frame MYC and V5 epitope tags (Fig. 1B). As shown in Fig. 1B, we do not observe specific protein signal from unintended reading frames. Blotting for the HA epitope tag for the polyQ frame yields clear protein signal, whereas blotting for MYC and V5 tags (alternative reading frames of the sense strand) does not yield signal above background, indicating that RAN translation is unlikely to be occurring with this design. We say “unlikely” since there is still the formal possibility of RAN from anti-sense frames, for which we were unable to generate in-frame tags. Nonetheless, based on the results in Fig. 1B and other similar data not included, as well as on prior work showing that CAGCAA repeats can circumvent RAN (Figura et al., 2015; Green et al., 2016; Li et al., 2008; Marti, 2016; Shieh and Bonini, 2011; Sobczak et al., 2003; Sobczak and Krzyzosiak, 2005; Stochmanski et al., 2012), we are confident that any RAN translation occurring from our constructs is likely negligible. We therefore proceeded with using the CAGCAA design to encode the polyQ of 80 repeats for both isoforms, which is within the range observed in the clinic (Costa Mdo and Paulson, 2012; Matos et al., 2019).

The new *Drosophila* lines were generated with the phiC31 site-specific integrase system, which enables insertion of a single construct in the same orientation at site attP2 on the third chromosome of *Drosophila* (Groth et al., 2004). The new ataxin-3 isoform 1 and 2 lines were verified for insertion at the proper site, in the same orientation and as a single copy through PCR, and were also sequence-verified from genomic DNA, as we have done routinely in the past (Tsou et al., 2015a,b, 2016). The phiC31 integrase system enables expression of transgenes at a similar level, as shown in Fig. 1C and as demonstrated in our prior work with other proteins and transgenes (Ristic et al., 2018; Sutton et al., 2017; Tsou et al., 2015a,b, 2016). Fig. 1D shows that the "start" and "end" genomic DNA sequencing results of the ataxin-3-encoding areas in the new fly lines are identical.

When we examine the protein levels of isoforms 1 and 2 when expressed in all fly neurons as well as in all fly tissues, we notice clear differences between the two. Even though at the mRNA level the two isoforms are similar and their "start" regions are the same (Fig. 1C and D), at the protein level they differ markedly. Isoform 1 protein is present at much higher levels than isoform 2 when expressed in all fly neurons (throughout development and in adults; Fig. 2A) as well as in all fly tissues (Fig. 2B). This difference is not due to the antibody used, as anti-HA blots show a similar difference between the two isoforms at the protein level (Supplemental fig. 1). The significantly lower levels of isoform 2 protein compared to isoform 1, coupled to our observations that their mRNA levels are similar, suggest that isoform 2 protein is degraded more rapidly in flies. This difference in protein levels between the two full-length ataxin-3 isoforms is not entirely unexpected, as prior work showed that isoform 2 is more rapidly degraded in cultured mammalian cells (Harris et al., 2010).

Next, we examined whether the two ataxin-3 isoforms are similarly partitioned in the nucleus and the cytoplasm. This is an important point since nuclear, pathogenic ataxin-3 is significantly more toxic than cytoplasmic ataxin-3 (Bichelmeier et al., 2007). Fig. 2C and Supplemental fig. 2 summarize our findings from cytoplasmic/nuclear fractionations: both isoforms are found similarly in these two fractions. With these new tools and an initial impression about their expression, protein levels and localization, we next investigated their toxicity in the fly.

3.2. Isoform 2 of pathogenic ataxin-3 is less toxic than isoform 1 in Drosophila

We assessed the toxicity of isoforms 1 and 2 of pathogenic ataxin-3 in *Drosophila* with the aid of several Gal4 drivers that we have employed in the past to examine the toxic properties of various proteins (Costa et al., 2016; Ristic et al., 2018; Sutton et al., 2017; Tsou et al., 2013; Tsou et al., 2015a,b, 2016). We began by expressing either isoform in all tissues, throughout fly development and in adults, *via* the sqh-Gal4 driver (Franke et al., 2010; Kiehart et al., 2004; Todi et al., 2005, 2008). As shown in Fig. 3A, ubiquitous expression of isoform 1 leads to developmental lethality: flies die during late pupal and early pharate adult stages, before they can emerge as adults. Expression of isoform 2 instead leads to successful eclosure of adults from their pupal cases; these flies survive for nearly 60 days. Control flies, which contain the sqh-Gal4 driver on the background of the chromosome targeted for

transgene insertion, live up to ~90 days. Co-expression of both isoforms in all tissues leads to a phenotype that is more severe than expression of isoform-1 alone (Supplemental fig. 3).

These data were corroborated by expression of either pathogenic ataxin-3 isoform in other tissues. As shown in Fig. 3B, expression of isoform 1 in all fly neurons, during development and in adults, leads to higher lethality than isoform 2. Flies expressing isoform 1 in all neurons successfully emerge as adults but die within one month. Isoform 2-expressing adults live for about 80 days and the control flies, which contain the elav-Gal4 driver, but without pathogenic ataxin-3 expression, die by ~100 days. Observations from longevity assays were complemented with motility tests, performed with the negative geotaxis assay. Through this method, adults in a vial are forced to the bottom by tapping and the number of flies that reach the top of the vial at 5, 15 and 30 s is calculated and expressed as a percentage of total flies in the vial. As shown in Fig. 3C, flies expressing isoform 1 panneuronally are impaired in their climbing ability compared to control flies and flies expressing isoform 2. Slower mobility from isoform 1-expressing flies is noticeable as early as day 7 and escalates throughout testing. Isoform 2-expressing flies also show reduced ability to climb, but later than isoform 1 counterparts. Still, for most of the time that we conducted this study, isoform 2 flies resembled controls (Fig. 3C).

Data from Fig. 3B and C were obtained using a pan-neuronal driver that expresses ataxin-3 isoforms throughout development and adulthood. We next assessed whether expression of either isoform in all fly neurons solely at adult stages shows a different pattern of lethality. The rationale behind this approach rests on the fact that SCA3 is an adultonset disease. What if the differential toxicity we observe with isoforms 1 and 2 of SCA3-causing ataxin-3 is due to developmental problems? We utilized a pan-neuronal driver, elav-Gal4-GS (Gene Switch), which requires the compound RU486 to initiate expression of ataxin-3 (Fig. 4A) (Nicholson et al., 2008; Roman et al., 2001; Sujkowski et al., 2015). Flies are raised in media without RU486. On day 1 after they emerge as adults, flies are placed in media with RU486 to induce protein expression (Blount et al., 2018; Ristic et al., 2018). Flies are then maintained in media with RU486 until they die and longevity is tracked daily. As summarized in Fig. 4B, expression of either isoform leads to increased lethality compared to controls, with lethality occurring earlier with isoform 1. Control flies contained the elav-Gal4-GS driver on the genetic background used to generate ataxin-3 lines.

Finally, we targeted either isoform to glial cells using the repo-Gal4 driver, which leads to transgene expression in development and adults. Here, we again notice markedly lower protein levels in glial cells for isoform 2 compared to isoform 1 (Fig. 4C). As shown in Fig. 4D, expression of isoform 1 again leads to accelerated incidence of death compared to expression of isoform 2; only a handful of adult flies from each independent cross is able to emerge and adults die within 12 days. Most isoform 1-expressing flies do not manage to eclose from their pupal cases. By contrast, isoform 2 is not more lethal to glial cells; adults that express isoform 2 only in glia emerge successfully as adults and live similarly to control adults that contain the Gal4 driver, but do not express pathogenic ataxin-3. Collectively, these observations demonstrate that isoform 1 of pathogenic ataxin-3 is significantly more toxic than isoform 2 in flies.

3.3. Aggregation of isoforms 1 and 2 of pathogenic ataxin-3 in flies

A defining property of pathogenic ataxin-3 is its propensity to aggregate (Costa Mdo and Paulson, 2012). This feature presents as macroinclusions in SCA3 mammalian brain and in cultured cells, its partitioning into soluble and insoluble (pellet) species through centrifugation protocols, and the retardation of aggregated species on filter-trap assays (Chang and Kuret, 2008; Matos et al., 2011, 2019; Ristic et al., 2018; Scherzinger et al., 1997, 1999; Weishaupl et al., 2019; Xu et al., 2002). We first utilized centrifugation to separate each isoform of pathogenic ataxin-3 into a pellet and soluble fraction. For this set of experiments, we used the elav-Gal4 driver to express either ataxin-3 isoform in all neuronal cells, and adults were collected on days 1, 7 and 14. Due to the much higher levels of isoform 1 protein than isoform 2, blots in Fig. 5A were imaged separately to avoid the need for over-exposure to obtain isoform 2 signal. We notice that each isoform of pathogenic ataxin-3 partitions both into soluble and pellet fractions on day 1 (Fig. 5A). However, unlike isoform 1, which by two weeks is mostly found in the pellet fraction, isoform 2 continues to be present in both fractions. At each time point more of isoform 1 fractionates into the pellet than isoform 2, indicating a higher aggregative propensity of this variant of the SCA3 protein (Fig. 5A). Another feature of isoform 1 that we do not observe as readily with isoform 2 is the clear presence of species at higher molecular weight (HMW) regions in the pellet fraction (denoted by black lines in Fig. 5A). These HMW smears are SDS-resistant species of pathogenic ataxin-3 that we have reported before and which accumulate in fly tissue (Ristic et al., 2018). Their unambiguous presence with isoform 1 underscores the higher propensity of isoform 1 to aggregate than isoform 2.

We next examined the aggregation of both isoforms through filter-retardation. We loaded samples of each isoform side by side (Fig. 5B) as well as separately (Fig. 5C) to show how much lower isoform 2 protein levels are compared to isoform 1 in this assay, similar to what we observe in other types of western blots. For quantification, however, we loaded preparations from both isoforms on separate filter papers and membranes, which were then processed simultaneously. Over the course of 14 days, we observe a clear and statistically significant increase in the amount of aggregated isoform 1 trapped on the membrane (Fig. 5B, C). We do not observe the same trend with isoform 2 over the same time course. In fact, we notice lower levels of filter-trapped species on days 7 and 14 compared to day 1 (Fig. 5C). Reduced levels of filter-trapped ataxin-3 isoform 2 from day 1 to day 7 could be due to different types of aggregates formed over time by isoform 1 compared to 2, as hinted at by the SDS-resistant smears in Fig. 5A. Future work, utilizing pure isoforms, is necessary to precisely differentiate the type of oligomeric and higher-order species that each isoform generates. At this point, we can conclude that over the course of two weeks in fly neurons we observe increased aggregation of pathogenic ataxin-3 isoform 1, but not of isoform 2, in two independent assays. Increased aggregation of isoform 1 over this time course could be due to the much lower protein levels of isoform 2—if there is less protein available to aggregate, quality control processes might more easily “handle” it, rendering the protein less toxic.

3.4. Isoform 2 at protein levels comparable to isoform 1 is no less toxic in Drosophila

Above, we observed that isoform 2 is much less toxic in flies than isoform 1 of pathogenic ataxin-3. This property of isoform 1 coincides with its higher protein levels. If both isoforms are expressed at the same protein level, is isoform 2 still less toxic to *Drosophila*? To address this question, we used fly genetics to express isoform 2 so that its protein levels are similar to isoform 1.

We used a different isoform 1-expressing fly line for these assays. As we showed in Fig. 3A, expression of isoform 1 in all tissues leads to developmental lethality. However, for work that we published before (Costa et al., 2016; Sutton et al., 2017) we prepared another fly line that expresses isoform 1 of pathogenic ataxin-3 at protein levels lower than the current transgene (this line is denoted as “weaker line” in Fig. 6A and Supplemental fig. 4). The ataxin-3-encoding transgene in this line is also inserted on the third chromosome of the fly and is on the same genetic background as the other two isoform lines described above. Flies expressing the “weaker” version of isoform 1 in all tissues can eclose as adults and survive for a number of days. We generated flies that contain one or two copies each of the driver and isoform 2 and used the sqh-Gal4 driver to examine their relative toxicity in all fly tissues. We selected this driver because ataxin-3 is a ubiquitously expressed protein and because in the above studies isoform 1 was consistently more potently toxic than isoform 2, regardless of expression pattern. Thus, we proceeded with ubiquitous expression for this set of investigations.

Increased copy number of driver and isoform 2 leads to higher isoform 2 protein levels (Fig. 6B) and increased lethality (Fig. 6C) compared to trans-heterozygous flies. Based on western blotting, double-homozygous driver;isoform 2 flies express ataxin-3 at protein levels comparable to the weaker isoform 1 (Fig. 6B). Flies that harbor two copies each of driver and transgene emerge as adults and survive for ~25 days. When we compare the longevity of these flies to those expressing the weaker isoform 1 line, we observe comparable survival curves (Fig. 6D; statistical analysis indicates that there is a significant difference in overall longevity of flies expressing isoform 2 compared to the weaker isoform 1-expressing line). Based on these results, isoform 2 is decidedly toxic in the fly when at protein levels similar to isoform 1.

3.5. Degradation of ataxin-3 by autophagy and the proteasome in Drosophila

Isoforms 1 and 2 mRNA levels are similar in the fly (Fig. 1C), but isoform 2 protein levels are much lower in all tissues tested (Figs. 2–6) suggesting that it is turned over more rapidly than isoform 1. The two major degradative routes in the cell are the proteasome and autophagy. We used fly genetics to examine the role of each pathway in determining the levels of ataxin-3. We expressed ataxin-3 isoform 1 or 2 by itself or in the presence of RNAi constructs targeting autophagy or proteasome components. For these analyses we limited expression to the eye, because knockdown of these genes more widely is lethal in flies, whereas targeting in fly eyes is tolerated ((Blount et al., 2018) and other observations from the Todi lab). Our findings from these assays are summarized quantitatively in Fig. 7A. Expression of isoform 2 in fly eyes results in lower protein levels compared to isoform 1 (Fig. 7B), similar to what we observe in all other fly tissues examined. Where available, we

used more than one RNAi line per gene, but in some cases we only had one line available. We reasoned that this approach is not unreasonable to explore the role of autophagy and the proteasome on isoform protein levels, since we are focusing on a general pathway rather than a specific gene.

For autophagy we targeted Atg7, Atg8a and Atg12, which are critical for the formation and expansion of the autophagosome (Otomo et al., 2013; Parzych and Klionsky, 2014). Atg8, a member of the ubiquitin-like proteins of the LC3 family, becomes conjugated to phosphatidylethanolamine at autophagosome-forming sites, where it plays a role in membrane dynamics and substrate recruitment (Otomo et al., 2013). Atg12 is constitutively conjugated to Atg5. The Atg12-Atg5 conjugate is essential for Atg8 lipidation and thus essential for autophagosome formation (Otomo et al., 2013; Parzych and Klionsky, 2014). We observe that targeting Atg12 and Atg8a though RNAi leads to a significant increase in protein levels for both isoforms (Fig. 7A and blots Fig. 7B–G). Overall, the effect is not very robust, ranging from 50%–100% increase in protein levels. These findings are limited to the effect from one RNAi line for each gene; results from the other RNAi line do not reach significance, probably due to differential capacity from each RNAi construct to reduce mRNA levels of the intended gene.

Next, we turned to the proteasome. The proteasome comprises a 20S degradative core and one or two 19S regulatory components (Amerik and Hochstrasser, 2004; Babbitt et al., 2005; Baumeister et al., 1998; Beck et al., 2012; VanderLinden et al., 2017). We focused on Rpn1 (part of the 19S, where it helps with proteasome substrate binding (Rosenzweig et al., 2012)) and the 20S proteolytic core components α5 and β2 (Amerik and Hochstrasser, 2004; Babbitt et al., 2005; Baumeister et al., 1998; Beck et al., 2012; VanderLinden et al., 2017). Targeting of each of these genes by RNAi leads to a statistically significant and robust increase in the protein levels of isoform 2, reaching as high as 400% (Fig. 7A, F, H, I). For isoform 1, targeting of Rpn1 and β2 also leads to higher protein levels (Fig. 7A, C, E). For Rpn1, three different RNAi lines lead to statistically increased protein levels for isoform 2, but only one line leads to higher levels for isoform 1 (Fig. 7A, C, E, F, H, I, J).

Collectively, we interpret these results to suggest that the proteasome and autophagy are both involved in the degradation of isoform 2 of pathogenic ataxin-3. The results are not as significant with isoform 1, but since targeting of at least one gene in each pathway leads to increased protein levels of this isoform as well, we are confident in concluding that isoform 1 is also a target of both pathways, in concurrence with prior reports (Costa Mdo and Paulson, 2012; Matos et al., 2011, 2019). Based on our observations, the proteasome is critically important for ataxin-3 degradation, with contribution from autophagy.

3.6. Isoform 2 is turned over more rapidly than isoform 1 in mammalian cells

All of our assays thus far employed an intact organism, the fruit fly. The isoforms we examined are of human origin and thus would benefit from investigations in a mammalian environment. We used the same constructs from fly-based work to examine the levels of both pathogenic ataxin-3 isoforms in mammalian cells. The objective for this next set of experiments was to determine whether isoform 2 of pathogenic ataxin-3 is degraded more rapidly than isoform 1 and whether the proteasome and autophagy are involved.

As shown in Fig. 8A, when either isoform is transiently transfected in HeLa cells, we observe much lower protein levels of isoform 2 than isoform 1. Inhibiting the proteasome (MG132) markedly increases the levels of isoform 2, approaching the protein levels of isoform 1 (Fig. 8A). Similarly, when we inhibit autophagy (chloroquine), we observe modestly, but statistically significantly increased levels of isoform 2 (Fig. 8B). We do not see a clear upregulation of isoform 1 in the presence of MG132 or chloroquine (Fig. 8A and B). This is likely because of the long half-life of ataxin-3 (Blount et al., 2014; Shoesmith Berke et al., 2005; Todi et al., 2007b) requiring prolonged incubation with inhibitors to observe an effect, as shown in Supplemental fig. 5.

We next determined that the lower levels of isoform 2 protein are due to its expedited degradation in cells. We inhibited new protein translation with cycloheximide (CHX). Isoform 1 is rather stable over the course of 6 h, whereas isoform 2 is degraded rapidly (Fig. 8C). Considering the strong effect of proteasome inhibition on the levels of isoform 2 (Fig. 8A), we examined whether MG132 halts the degradation of isoform 2. As shown in Fig. 8C, in the presence of MG132 degradation of isoform 2 is essentially halted.

The experiments above were conducted in HeLa cells. We conducted similar studies in HEK-293 T cells in order to recapitulate our findings in another mammalian cell line. Again, we observe lower levels of isoform 2 than isoform 1 (Supplemental fig. 6), mirroring the results we observed in HeLa cells (Fig. 8A–C). Proteasome inhibition has a strong impact on the levels of isoform 2, whereas application of chloroquine does not lead to noticeable changes in its protein levels. As in HeLa cells, we again observe that isoform 1 is not readily impacted by the application of proteasome or autophagy inhibitors in HEK-293 T cells. Based on these results, we conclude that isoform 2 is degraded more rapidly by the proteasome than isoform 1 in mammalian cells, with additional, minor contribution from autophagy.

3.7. The role of the C-terminus in the stability of isoform 2

The only difference between the two ataxin-3 isoforms is at their C-termini, and isoform 2 is degraded decidedly more rapidly than isoform 1. Rapid turnover of isoform 2 could be due to the recognition of its tail end by degradative machineries, with its C-terminus essentially functioning as a degron (amino acid sequences that signal host protein turnover). Degron sequences function alone or in conjunction with internal lysine residues that enable their ubiquitination to target host proteins for degradation, and can be found at either terminus or internally in a protein (Cho and Dreyfuss, 2010; Fortmann et al., 2015; Varshavsky, 2019). If the tail of isoform 2 acts as a degron, then its addition to isoform 1 should lead to lower protein levels. It is also possible that the C-terminus of isoform 1 instead stabilizes its host protein; thus, its fusion onto isoform 2 might increase its protein levels.

We fused the C-terminus of isoform 1 onto the end of isoform 2 and *vice versa* (Fig. 9A). As shown in Fig. 9B, C and F, addition of the C-terminus of isoform 1 onto isoform 2 leads to higher levels of this protein in a proteasome-dependent manner; autophagy does not seem critical. The levels of the new construct now approach those of isoform 1 (Fig. 9B, C and F), and are much higher than the levels of the original isoform 2. Conversely, fusion of the C-terminus of isoform 2 to the end of isoform 1 leads to significantly lower protein levels (Fig.

9D, E); the new resulting protein is at levels comparable to those of isoform 2 (Fig. 9F). Proteasome inhibition results in higher levels of isoform 1 with the C-terminus of isoform 2 (Fig. 9D, F); autophagy again does not seem to have a noticeable impact (Fig. 9E, F).

From these assays, it appears that the C-terminus of isoform 2 has a destabilizing effect on its host protein. At the same time, the C-terminus of isoform 1 might also protect ataxin-3 protein from degradation. The current setup does not entirely exclude the possibility that the stabilizing effect of the C-terminus of isoform 1 onto isoform 2 prevents the recognition of the tail-end of isoform 2 as a potential degron. It should be noted, however, that all of the ataxin-3 constructs used here are capped by an HA epitope tag at their C-termini (Fig. 9A); if the C-terminus of isoform 2 must be at the very tail-end of ataxin-3 to destabilize it, then the HA tag should have also precluded its recognition for degradation and would have presumably led to protein levels comparable to isoform 1. Thus, it is still possible that the C-terminus of isoform 1 has a stabilizing effect on the rest of ataxin-3. Altogether, these data suggest that the C-terminus of ataxin-3 is important for the overall levels of the SCA3 protein, unlocking new paths to consider for the handling of this protein in the cellular environment.

4. Discussion

The work presented here sheds new light on the relative pathogenic contribution of the two major ataxin-3 isoforms in SCA3. Two full-length ataxin-3 protein variants arise from alternative splicing of the *ATXN3* gene, in which the abnormal expansion of a polyQ-encoding CAG triplet repeat causes SCA3. Each isoform contains the same N-terminal portion and polyQ domain, but differs at the C-terminus. The objective of this study was to investigate the possibility of differential toxicity from the two main, full-length isoforms that are expressed in the mammalian brain. Our fly-based investigations show that polyQ-expanded isoform 2 is less toxic than polyQ-expanded isoform 1, as a result of lower protein levels. Isoform 2 is more rapidly degraded, principally by the proteasome, leading to reduced aggregative propensity and toxicity in all fly tissues tested. Thus, polyQ-expanded isoform 2 of pathogenic ataxin-3 is not likely to be a major contributor to SCA3. (We note here that expression of ataxin-3 with a normal repeat of 22–25Q is not toxic when present throughout the fly or in select tissues, *e.g.* neuronal, eye or glial, using the same drivers as in this work; (Tsou et al., 2013, 2015a,b) and additional, unpublished observations by the Todi lab.)

Prior work with isoforms 1 and 2 *in vitro* and in mammalian cells observed higher aggregation of isoform 2 than isoform 1 (Harris et al., 2010), which differs from what we observe in flies. The tail of isoform 2 is inherently more hydrophobic than that of isoform 1 (Harris et al., 2010), most likely accounting for its enhanced aggregation in the earlier study. However, the isoforms might behave differently in an intact organism, leading to higher aggregation of isoform 1 than 2. Another key point that may explain this difference is the fact that isoform 2 is present at much lower protein levels in fly models, thus presenting a reduced challenge for quality control pathways that regulate its folding and aggregation. There may also be cell type- and tissue-specific differences in the aggregative propensity of one isoform over the other in the mammalian brain. Addressing this last point will require

the generation of additional tools that can reliably and consistently identify one species over the other in the mammalian brain. Based on our work in fly neurons, we can only conclude that the two isoforms behave differently, with isoform 1 more likely to aggregate than isoform 2.

A recent study investigated ataxin-3 isoform properties in cultured mammalian cells (HEK-293T) by utilizing *ATXN3* knockout cells and transiently expressing the ataxin-3 isoforms described here (Weishaupl et al., 2019). This other work included yet another variant of ataxin-3 with a premature stop codon in isoform 2 (Fig. 1A), a variant which we did not investigate, choosing instead to focus on the full-length proteins for this manuscript. Both versions of isoform 2 (early-stop and full-length) exist in SCA3 patients. Results from this prior publication do not mirror our observations: it concluded that full-length isoforms 1 and 2 harboring the polyQ expansion are degraded similarly in HEK-293T cells and that autophagy, rather than the proteasome, primarily mediates their turnover (Weishaupl et al., 2019). Instead, we observe clear proteasome involvement and rapid degradation rates for isoform 2 compared to 1. Supporting the present observations, an earlier investigation also found that isoform 2 is more rapidly cleared in a proteasome-dependent manner in cultured mammalian cells (Harris et al., 2010). How might we resolve these differences? Autophagy likely participates in the degradation of pathogenic ataxin-3 and has been reported before as a key component in ridding the cell of the SCA3 protein (Ashkenazi et al., 2017; Costa Mdo and Paulson, 2012; Matos et al., 2011, 2019; Nobrega et al., 2018; Sittler et al., 2018). Depending on specific conditions and types of stress, one pathway may pre-dominate over the other in importance for ataxin-3 degradation. With respect to the degradation rates of each isoform, our overall results and prior published work (Harris et al., 2010) lead us to propose that under most cases isoform 2 is less stable than isoform 1 of pathogenic ataxin-3, regardless of the mechanism of clearance.

Our work raises an intriguing question: what property of isoform 2 renders it more rapidly degraded? We suggest that the C-terminus of isoform 2 acts as a degron, signaling the degradation of the host protein. Whether the tail of isoform 2 is directly recognized by degradative machineries as a signal, or whether its ubiquitination is required for the protein to be eliminated, awaits determination. We have shown before that ataxin-3 does not require its own ubiquitination to be degraded (Blount et al., 2014); it may well be that the C-terminus of isoform 2 directly targets the host protein to the proteasome through specific protein-protein interactions. Our studies also posit the additional possibility that the C-terminus of isoform 1 stabilizes its host protein. The tail of isoform 1 could protect the rest of the protein from degradation through specific binding partners that preclude the degradation of ataxin-3, similar to what we have observed for ataxin-3 and Rad23 (Blount et al., 2014; Sutton et al., 2017). As found in work by other scientists (Weishaupl et al., 2019), the two different C-termini of ataxin3 have differing binding partners—*e.g.* ubiquitin can bind the tail of isoform 1 but not isoform 2 due to the lack of UIM3—that may dictate their stability and functions. Additional explorations into the precise nature of isoform 2 degradation may find new mechanisms of protein quality control that could be of importance not only to understand SCA3, but also more generally the principles guiding protein turnover in this and other diseases.

In conclusion, we investigated whether the two full-length ataxin-3 isoforms are differentially toxic *in vivo* when harboring a disease-range polyQ repeat. Our results reveal marked differences in isoform toxicity due to differences in the stability of the two variants of the SCA3 protein. Defining the properties and propensities of various products expressed by a disease gene, as done here for SCA3, is necessary to comprehend how that disease arises and how to treat it.

Supplementary Material

Refer to Web version on PubMed Central for supplementary material.

Acknowledgments

Funding

This work was funded by a Wayne State University Graduate Research Fellowship to SLJ, by a Wayne State University Thomas Rumble Fellowship to JRB, by R01NS038712 to HLP from NINDS, by a Pilot Grant Award to SVT from the Department of Pharmacology at Wayne State University, by a Pioneer in SCA Award to SVT from the National Ataxia Foundation, and by R01NS086778 to SVT from NINDS.

Abbreviations

DUB	deubiquitinase
HMW	higher molecular weight
MJD	Machado-Joseph disease
PolyQ	polyglutamine
SCA	Spinocerebellar Ataxia
UAS	upstream activating sequence
UIM	ubiquitin-interacting motif

References

Amerik AY, Hochstrasser M, 2004 Mechanism and function of deubiquitinating enzymes. Biochim. Biophys. Acta 1695, 189–207. [PubMed: 15571815]

Ashkenazi A, et al., 2017 Polyglutamine tracts regulate beclin 1-dependent autophagy. Nature. 545, 108–111. [PubMed: 28445460]

Babbitt SE, et al., 2005 ATP hydrolysis-dependent disassembly of the 26S proteasome is part of the catalytic cycle. Cell. 121, 553–565. [PubMed: 15907469]

Banez-Coronel M, et al., 2015 RAN translation in Huntington disease. Neuron. 88, 667–677. [PubMed: 26590344]

Baumeister W, et al., 1998 The proteasome: paradigm of a self-compartmentalizing protease. Cell. 92, 367–380. [PubMed: 9476896]

Beck F, et al., 2012 Near-atomic resolution structural model of the yeast 26S proteasome. Proc. Natl. Acad. Sci. U. S. A 109, 14870–14875. [PubMed: 22927375]

Bettencourt C, et al., 2010 Increased transcript diversity: novel splicing variants of Machado-Joseph disease gene (ATXN3). Neurogenetics. 11, 193–202. [PubMed: 19714377]

Bichelmeier U, et al., 2007 Nuclear localization of ataxin-3 is required for the manifestation of symptoms in SCA3: in vivo evidence. J. Neurosci 27, 7418–7428. [PubMed: 17626202]

Blount JR, et al., 2014 Ubiquitin-binding site 2 of ataxin-3 prevents its proteasomal degradation by interacting with Rad23. Nat. Commun 5, 4638. [PubMed: 25144244]

Blount JR, et al., 2018 Expression and regulation of deubiquitinase-resistant, unanchored ubiquitin chains in drosophila. Sci. Rep 8, 8513. [PubMed: 29855490]

Brand AH, Perrimon N, 1993 Targeted gene expression as a means of altering cell fates and generating dominant phenotypes. Development. 118, 401–415. [PubMed: 8223268]

Buijsen RAM, et al., 2019 Genetics, mechanisms, and therapeutic progress in polyglutamine spinocerebellar ataxias. Neurother. 16 (2), 263–286.

Chang E, Kuret J, 2008 Detection and quantification of tau aggregation using a membrane filter assay. Anal. Biochem 373, 330–336. [PubMed: 17949677]

Cho S, Dreyfuss G, 2010 A degron created by SMN2 exon 7 skipping is a principal contributor to spinal muscular atrophy severity. Genes Dev. 24, 438–442. [PubMed: 20194437]

Costa MD, Paulson HL, 2012 Toward understanding Machado-Joseph disease. Prog. Neurobiol 97, 239–257. [PubMed: 22133674]

Costa MD, et al., 2016 Unbiased screen identifies aripiprazole as a modulator of abundance of the polyglutamine disease protein, ataxin-3. Brain. 139 (11), 2891–2908. [PubMed: 27645800]

Figura G, et al., 2015 In vitro expansion of CAG, CAA, and mixed CAG/CAA repeats. Int. J. Mol. Sci 16, 18741–18751. [PubMed: 26270660]

Fortmann KT, et al., 2015 A regulated, ubiquitin-independent Degron in IkappaBalpha. J. Mol. Biol 427, 2748–2756. [PubMed: 26191773]

Franke JD, et al., 2010 Nonmuscle myosin II is required for cell proliferation, cell sheet adhesion and wing hair morphology during wing morphogenesis. Dev. Biol 345, 117–132. [PubMed: 20599890]

Goto J, et al., 1997 Machado-Joseph disease gene products carrying different carboxyl termini. Neurosci. Res 28, 373–377. [PubMed: 9274833]

Green KM, et al., 2016 RAN translation-what makes it run? Brain Res. 1647, 30–42. [PubMed: 27060770]

Groth AC, et al., 2004 Construction of transgenic Drosophila by using the site-specific integrase from phage phiC31. Genetics. 166, 1775–1782. [PubMed: 15126397]

Harris GM, et al., 2010 Splice isoforms of the polyglutamine disease protein ataxin-3 exhibit similar enzymatic yet different aggregation properties. PLoS One 5, e13695. [PubMed: 21060878]

Ichikawa Y, et al., 2001 The genomic structure and expression of MJD, the MachadoJoseph disease gene. J. Hum. Genet 46, 413–422. [PubMed: 11450850]

Kawaguchi Y, et al., 1994 CAG expansions in a novel gene for Machado-Joseph disease at chromosome 14q32.1. Nat. Genet 8, 221–228. [PubMed: 7874163]

Kiehart DP, et al., 2004 Drosophila crinkled, mutations of which disrupt morphogenesis and cause lethality, encodes fly myosin VIIA. Genetics. 168, 1337–1352. [PubMed: 15579689]

La Spada AR, Taylor JP, 2003 Polyglutamines placed into context. Neuron. 38, 681–684. [PubMed: 12797953]

Li LB, et al., 2008 RNA toxicity is a component of ataxin-3 degeneration in Drosophila. Nature. 453, 1107–1111. [PubMed: 18449188]

Lieberman AP, et al., 2019 1 24 Polyglutamine repeats in neurodegenerative diseases. Annu. Rev. Pathol 14, 1–27 (Epub 2018 Aug 8). [PubMed: 30089230]

Marti E, 2016 RNA toxicity induced by expanded CAG repeats in Huntington's disease. Brain Pathol. 26, 779–786. [PubMed: 27529325]

Matos CA, et al., 2011 Polyglutamine diseases: the special case of ataxin-3 and Machado-Joseph disease. Prog. Neurobiol 95, 26–48. [PubMed: 21740957]

Matos CA, et al., 2019 Machado-Joseph disease/spinocerebellar ataxia type 3: lessons from disease pathogenesis and clues into therapy. J. Neurochem 148 (1), 8–28 (Epub 2018 Oct 5). [PubMed: 29959858]

Nicholson L, et al., 2008 Spatial and temporal control of gene expression in Drosophila using the inducible GeneSwitch GAL4 system. I. Screen for larval nervous system drivers. Genetics. 178, 215–234. [PubMed: 18202369]

Nobrega C, et al., 2018 Molecular mechanisms and cellular pathways implicated in Machado-Joseph disease pathogenesis. Adv. Exp. Med. Biol 1049, 349–367. [PubMed: 29427113]

Otomo C, et al., 2013 Structure of the human ATG12~ATG5 conjugate required for LC3 lipidation in autophagy. Nat. Struct. Mol. Biol 20, 59–66. [PubMed: 23202584]

Parzych KR, Klionsky DJ, 2014 An overview of autophagy: morphology, mechanism, and regulation. Antioxid. Redox Signal 20, 460–473. [PubMed: 23725295]

Paulson HL, et al., 1997a Machado-Joseph disease gene product is a cytoplasmic protein widely expressed in brain. Ann. Neurol 41, 453–462. [PubMed: 9124802]

Paulson HL, et al., 1997b Intranuclear inclusions of expanded polyglutamine protein in spinocerebellar ataxia type 3. Neuron. 19, 333–344. [PubMed: 9292723]

Paulson HL, et al., 2017 Polyglutamine spinocerebellar ataxias - from genes to potential treatments. Nat. Rev. Neurosci 18, 613–626. [PubMed: 28855740]

Ristic G, et al., 2018 Toxicity and aggregation of the polyglutamine disease protein, ataxin-3 is regulated by its binding to VCP/p97 in Drosophila melanogaster. Neurobiol. Dis 116, 78–92. [PubMed: 29704548]

Roman G, et al., 2001 P[Switch], a system for spatial and temporal control of gene expression in Drosophila melanogaster. Proc. Natl. Acad. Sci. U. S. A 98, 12602–12607. [PubMed: 11675496]

Rosenzweig R, et al., 2012 Rpn1 and Rpn2 coordinate ubiquitin processing factors at proteasome. J. Biol. Chem 287, 14659–14671. [PubMed: 22318722]

Scherzinger E, et al., 1997 Huntingtin-encoded polyglutamine expansions form amyloid-like protein aggregates in vitro and in vivo. Cell. 90, 549–558. [PubMed: 9267034]

Scherzinger E, et al., 1999 Self-assembly of polyglutamine-containing huntingtin fragments into amyloid-like fibrils: implications for Huntington's disease pathology. Proc. Natl. Acad. Sci. U. S. A 96, 4604–4609. [PubMed: 10200309]

Schmidt T, et al., 1998 An isoform of ataxin-3 accumulates in the nucleus of neuronal cells in affected brain regions of SCA3 patients. Brain Pathol. 8, 669–679. [PubMed: 9804376]

Schmitt I, et al., 2007 Inactivation of the mouse Atxn3 (ataxin-3) gene increases protein ubiquitination. Biochem. Biophys. Res. Commun 362, 734–739. [PubMed: 17764659]

Shieh SY, Bonini NM, 2011 Genes and pathways affected by CAG-repeat RNA-based toxicity in Drosophila. Hum. Mol. Genet 20, 4810–4821. [PubMed: 21933837]

Shoesmith Berke SJ, et al., 2005 Defining the role of ubiquitin interacting motifs in the polyglutamine disease protein, ataxin-3. J. Biol. Chem 280, 32026–32034. [PubMed: 16040601]

Sittler A, et al., 2018 Deregulation of autophagy in postmortem brains of MachadoJoseph disease patients. Neuropathology. 38, 113–124. [PubMed: 29218765]

Sobczak K, Krzyzosiak WJ, 2005 CAG repeats containing CAA interruptions form branched hairpin structures in spinocerebellar ataxia type 2 transcripts. J. Biol. Chem 280, 3898–3910. [PubMed: 15533937]

Sobczak K, et al., 2003 RNA structure of trinucleotide repeats associated with human neurological diseases. Nucleic Acids Res. 31, 5469–5482. [PubMed: 14500809]

Stochmanski SJ, et al., 2012 Expanded ATXN3 frameshifting events are toxic in Drosophila and mammalian neuron models. Hum. Mol. Genet 21, 2211–2218. [PubMed: 22337953]

Sujkowski A, et al., 2015 Endurance exercise and selective breeding for longevity extend Drosophila healthspan by overlapping mechanisms. Aging (Albany NY) 7, 535–552. [PubMed: 26298685]

Sutton JR, et al., 2017 Interaction of the polyglutamine protein ataxin-3 with Rad23 regulates toxicity in Drosophila models of Spinocerebellar Ataxia Type 3. Hum Mol Genet. 26 (8), 1419–1431. [PubMed: 28158474]

Switonski PM, et al., 2011 Mouse ataxin-3 functional knock-out model. NeuroMolecular Med. 13, 54–65. [PubMed: 20945165]

Todi SV, et al., 2005 Myosin VIIA defects, which underlie the usher 1B syndrome in humans, lead to deafness in Drosophila. Curr. Biol 15, 862–868. [PubMed: 15886106]

Todi SV, et al., 2007a Polyglutamine repeat disorders, including Huntington's disease In: Waxman SG (Ed.), Molecular Neurology. Academic Press, London, pp. 257–276.

Todi SV, et al., 2007b Cellular turnover of the polyglutamine disease protein ataxin-3 is regulated by its catalytic activity. J. Biol. Chem 282, 29348–29358. [PubMed: 17693639]

Todi SV, et al., 2008 Myosin VIIA, important for human auditory function, is necessary for Drosophila auditory organ development. PLoS One 3, e2115. [PubMed: 18461180]

Todi SV, et al., 2009 Ubiquitination directly enhances activity of the deubiquitinating enzyme ataxin-3. EMBO J. 28, 372–382. [PubMed: 19153604]

Todi SV, et al., 2010 Activity and cellular functions of the deubiquitinating enzyme and polyglutamine disease protein ataxin-3 are regulated by ubiquitination at lysine 117. J. Biol. Chem 285, 39303–39313. [PubMed: 20943656]

Tsou WL, et al., 2013 Ubiquitination regulates the neuroprotective function of the deubiquitinase ataxin-3 in vivo. J. Biol. Chem 288, 34460–34469. [PubMed: 24106274]

Tsou WL, et al., 2015a The deubiquitinase ataxin-3 requires Rad23 and DnaJ-1 for its neuroprotective role in Drosophila melanogaster. Neurobiol. Dis 82, 12–21. [PubMed: 26007638]

Tsou WL, et al., 2015b DnaJ-1 and karyopherin alpha-3 suppress degeneration in a new Drosophila model of Spinocerebellar Ataxia Type 6. Hum Mol Genet. 24 (15), 4385–4396 (Epub 2015 May 7). [PubMed: 25954029]

Tsou WL, et al., 2016 Polyglutamine length-dependent toxicity from alpha1ACT in Drosophila models of spinocerebellar ataxia type 6. Biol Open. 5, 1770–1775. [PubMed: 27979829]

VanderLinden RT, et al., 2017 Structure and energetics of pairwise interactions between proteasome subunits RPN2, RPN13, and ubiquitin clarify a substrate recruitment mechanism. J. Biol. Chem 292, 9493–9504. [PubMed: 28442575]

Varshavsky A, 2019 N-degron and C-degron pathways of protein degradation. Proc. Natl. Acad. Sci. U. S. A 116, 358–366. [PubMed: 30622213]

Warrick JM, et al., 2005 Ataxin-3 suppresses polyglutamine neurodegeneration in Drosophila by a ubiquitin-associated mechanism. Mol. Cell 18, 37–48. [PubMed: 15808507]

Weishaupl D, et al., 2019 Physiological and pathophysiological characteristics of ataxin-3 isoforms. J. Biol. Chem 294, 644–661. [PubMed: 30455355]

Winborn BJ, et al., 2008 The deubiquitinating enzyme ataxin-3, a polyglutamine disease protein, edits Lys63 linkages in mixed linkage ubiquitin chains. J. Biol. Chem 283, 26436–26443. [PubMed: 18599482]

Xu G, et al., 2002 Rapid detection of protein aggregates in the brains of Alzheimer patients and transgenic mouse models of amyloidosis. Alzheimer Dis. Assoc. Disord 16, 191–195. [PubMed: 12218651]

Zeng L, et al., 2013 The de-ubiquitinating enzyme ataxin-3 does not modulate disease progression in a knock-in mouse model of Huntington disease. J Huntingtons Dis. 2, 201–215. [PubMed: 24683430]

Zoghbi HY, Orr HT, 2000 Glutamine repeats and neurodegeneration. Annu. Rev. Neurosci 23, 217–247. [PubMed: 10845064]

Zoghbi HY, Orr HT, 2009 Pathogenic mechanisms of a polyglutamine-mediated neurodegenerative disease, spinocerebellar ataxia type 1. J. Biol. Chem 284, 7425–7429. [PubMed: 18957430]

Zu T, et al., 2011 Non-ATG-initiated translation directed by microsatellite expansions. Proc. Natl. Acad. Sci. U. S. A 108, 260–265. [PubMed: 21173221]

Zu T, et al., 2018 Repeat-associated non-ATG translation in neurological diseases. Cold Spring Harb. Perspect. Biol 10 (12) (pii: a033019). [PubMed: 29891563]

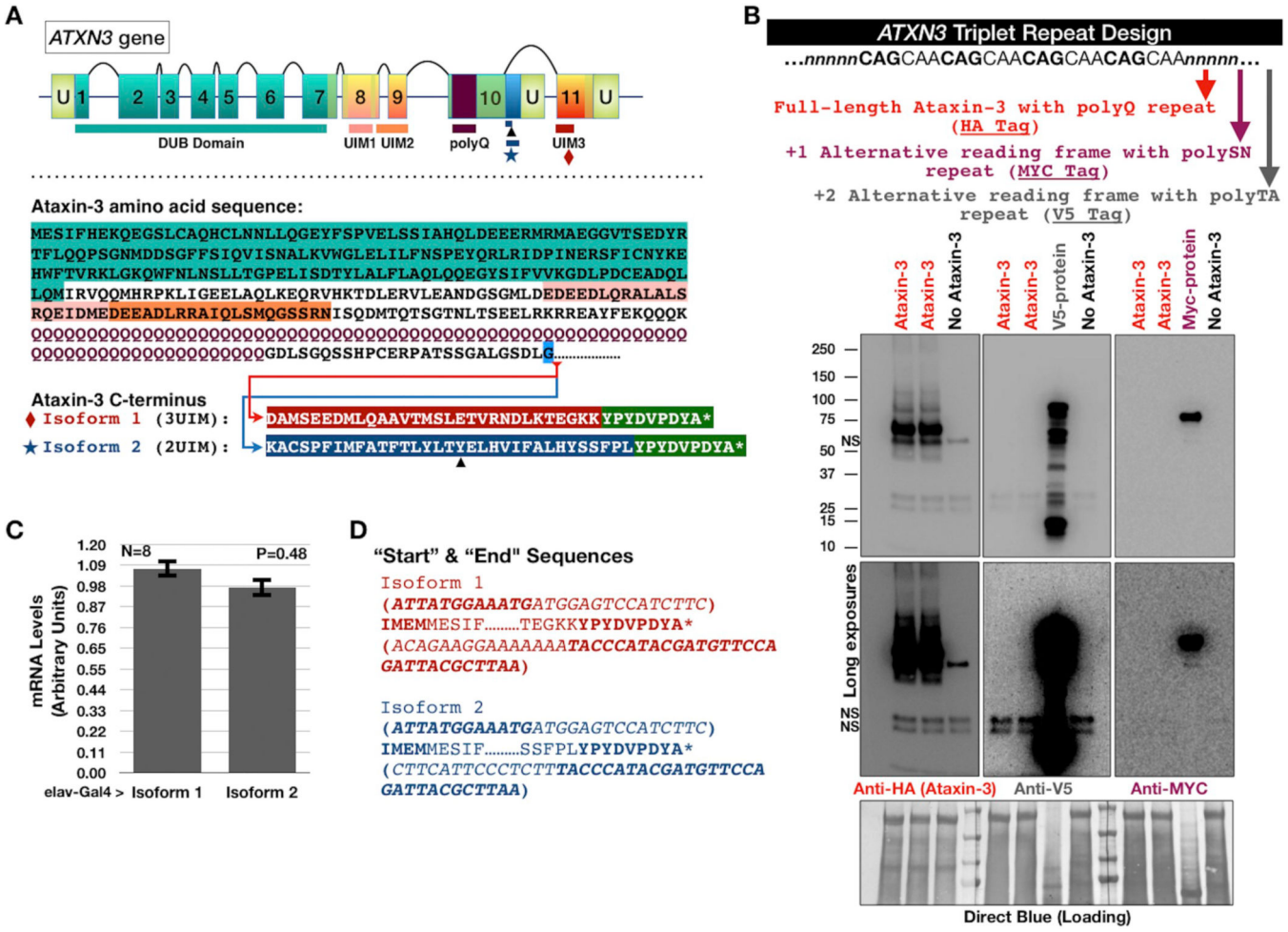

Fig. 1. New *Drosophila* lines for SCA3.

A) *ATXN3* isoforms. U: untranslated region; DUB: deubiquitinase; polyQ: polyglutamine; UIM: ubiquitin-interacting motif. 2-UIM transcript is termed here isoform 2 since it is less common (Harris et al., 2010). Isoform 1 results from alternative splicing linking exon 10 to 11 for UIM3 (♦). (★) Isoform 2 with a different tail, lacking UIM3. (▲) A SNP results in an early stop within isoform 2. In this work, both isoforms are capped by an HA tag.

B) Ataxin-3 constructs were designed with a CAGCAA repeat to encode polyQ. PolyQ frame is HA-tagged. Isoform 1 is shown. The other, non-polyQ sense frames are MYC and V5 tagged. NS: non-specific.

C) qRT-PCR from adults expressing either isoform in all neurons. Means ± SEM. *P* value from student's *t*-test. Flies were one day old.

D) Start and end sequences for the ataxin-3 lines from genomic sequencing. Italics: nucleotides. Sequence between nucleotides is ataxin-3 amino acid sequence. Bold: sequences added for Kozak (front) and HA tag (end).

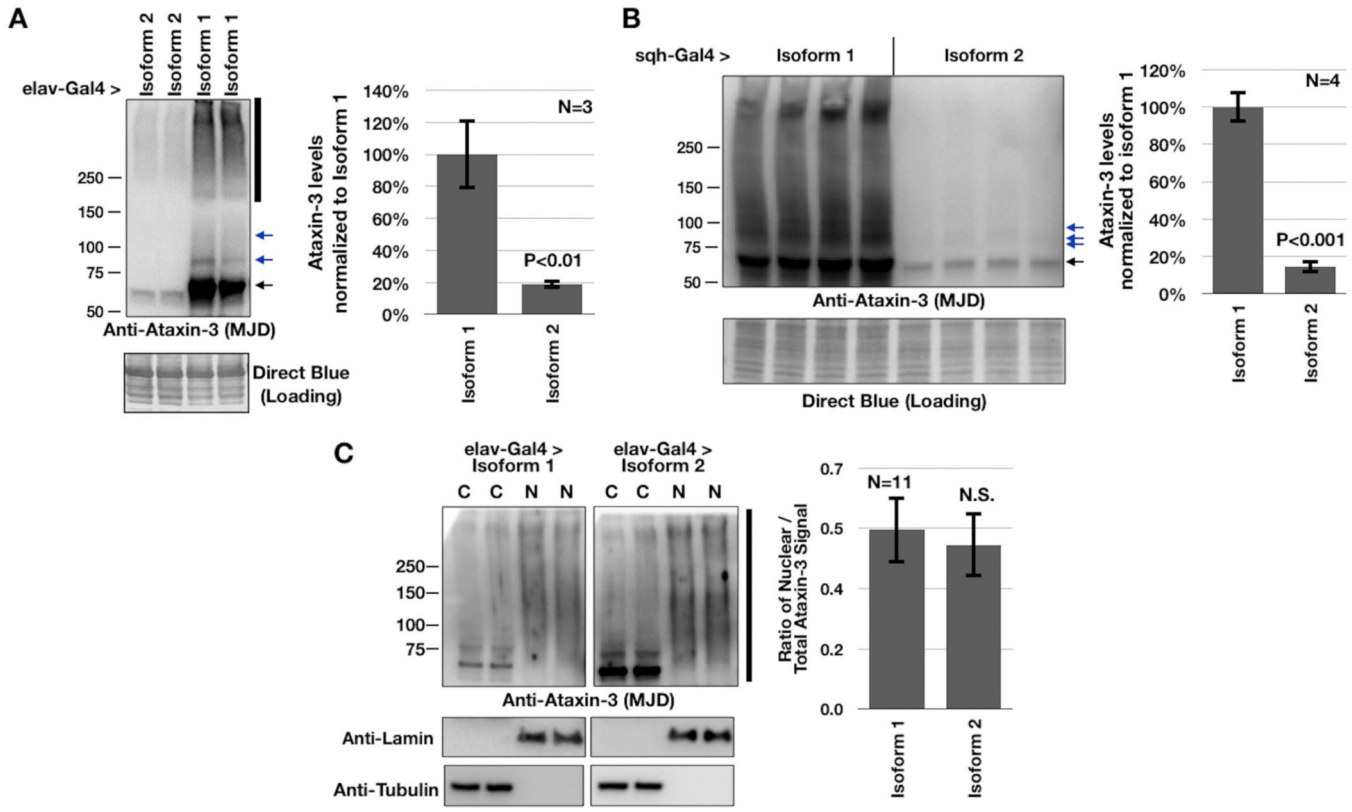

Fig. 2. Expression of the two ataxin-3 isoforms in flies.

A & B) Western blots when isoforms are expressed in all neurons (A) or ubiquitously (B). Adults were used for panel A and pupae for panel B. For quantification, the entire signal in each lane was used. Means ± SD. *P* values from student's *t*-tests. Black arrow: unmodified ataxin-3. Blue arrows: ubiquitinated ataxin-3 (Todi et al., 2007b, 2009, 2010; Tsou et al., 2013). Black bar: SDS-resistant species. In all blots, isoform 2 migrates slightly lower than isoform 1.

C) Western blots from cytoplasmic (C) / nuclear (N) separation of fly lysates expressing isoforms in all neurons. The entire signal - the main band as well as smear above it - was quantified, as denoted by the bar on the right side of the blots. Isoforms were loaded on separate gels to avoid over-exposure. Means ± SD. N.S.: non-significant *P* value from student's *t*-test. Flies were one day old. (For interpretation of the references to colour in this figure legend, the reader is referred to the web version of this article.)

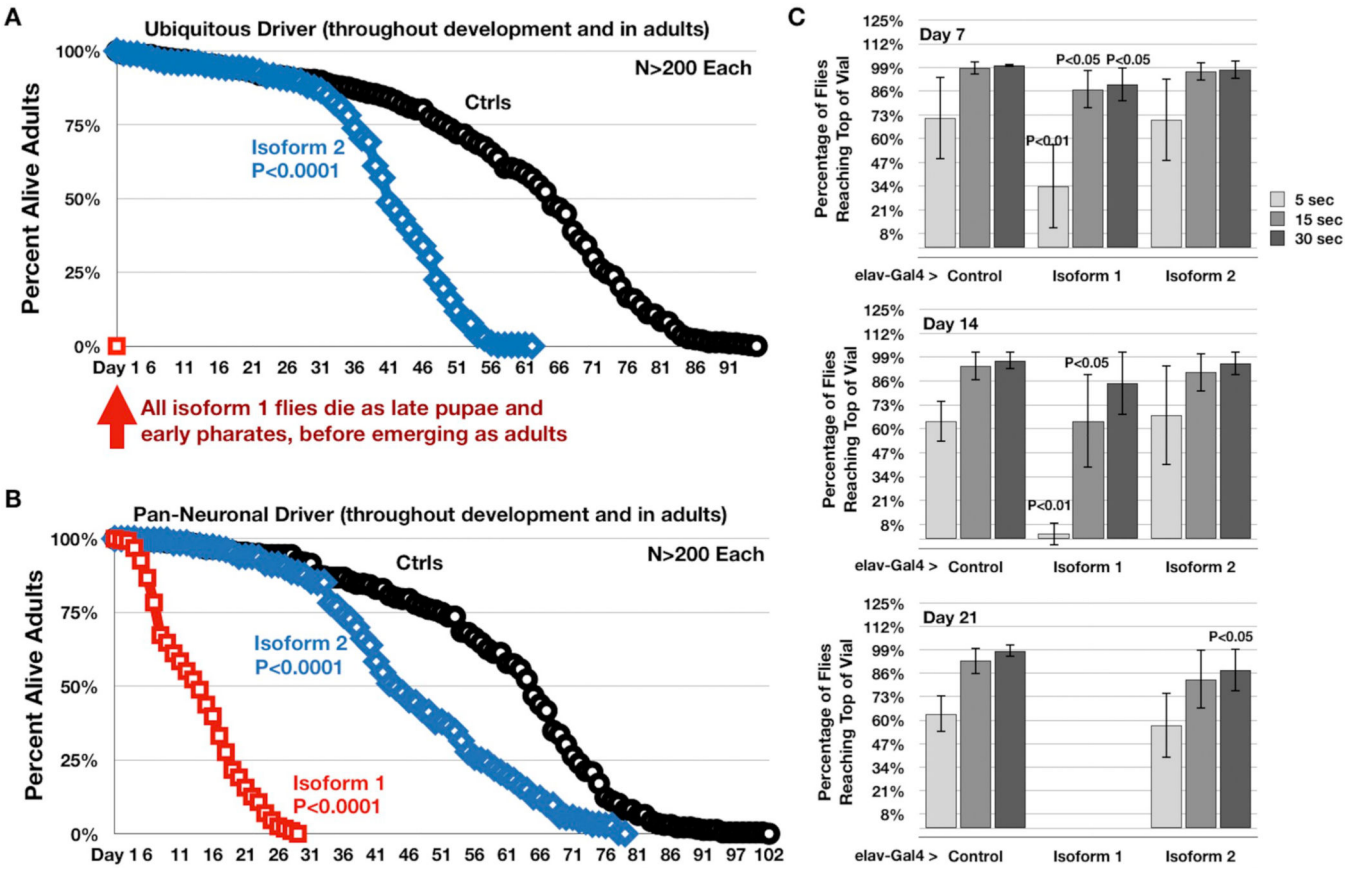

Fig. 3. Differential toxicity from pathogenic ataxin-3 isoforms in developing and adult flies.

A & B) Adult fly longevity when isoform 1 or 2 of pathogenic ataxin-3 was expressed in the noted tissues. Ubiquitous driver was sqh-Gal4, pan-neuronal driver was elav-Gal4. *P* values from log-rank tests.

C) Negative geotaxis assays of flies with the noted genotypes. *P* values from student's *t*-tests comparing motility of isoforms 1 and 2 to control flies for their respective time course. None of the flies set aside for motility assays for isoform 1 survived to day 21. At least 50 flies per group were used.

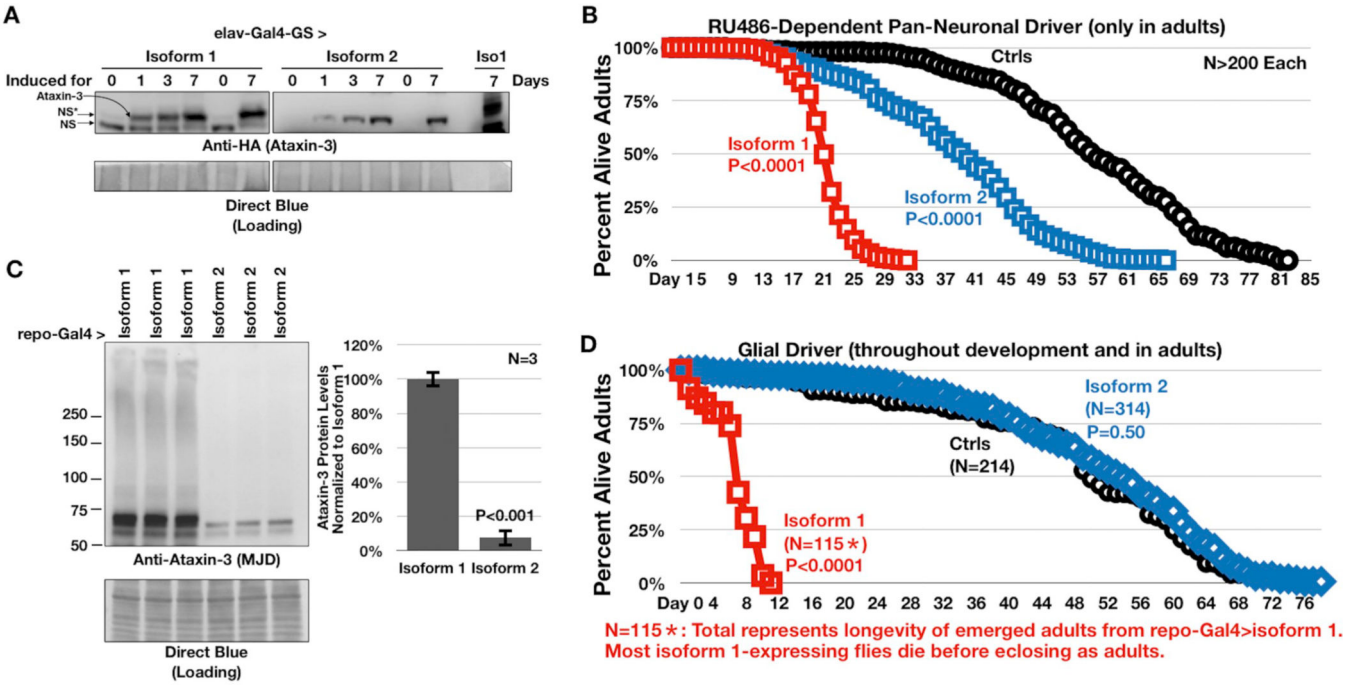

Fig. 4. Differential toxicity from pathogenic ataxin-3 isoforms in adult neurons and in glia.

A) Western blots from whole fly lysates. Flies heterozygous for both elav-Gal4-GS driver and either isoform were raised in media without RU486 until they emerged as adults, when they were placed in RU486-containing media for the indicated amount of time. NS: non-specific bands we sometimes observe with the indicated antibody. NS*: another non-specific band present only in lanes 1 and 5, running immediately below/near the ataxin-3-positive band. In the isoform 2 blot, 4/5th less lysate was loaded for isoform 1 compared to the other lanes. Iso: isoform.

B, D) Adult fly longevity when isoform 1 or 2 of pathogenic ataxin-3 was expressed in the noted tissues. Pan-neuronal driver dependent on RU486 was elav-Gal4-GS, and glial cell driver was repo-Gal4. *P* values from log-rank tests.

C) Western blots from adult flies expressing isoform 1 or 2, driven by repo-Gal4. Shown in histograms are means ± SD. *P* value from student's *t*-test. Flies were one day old.

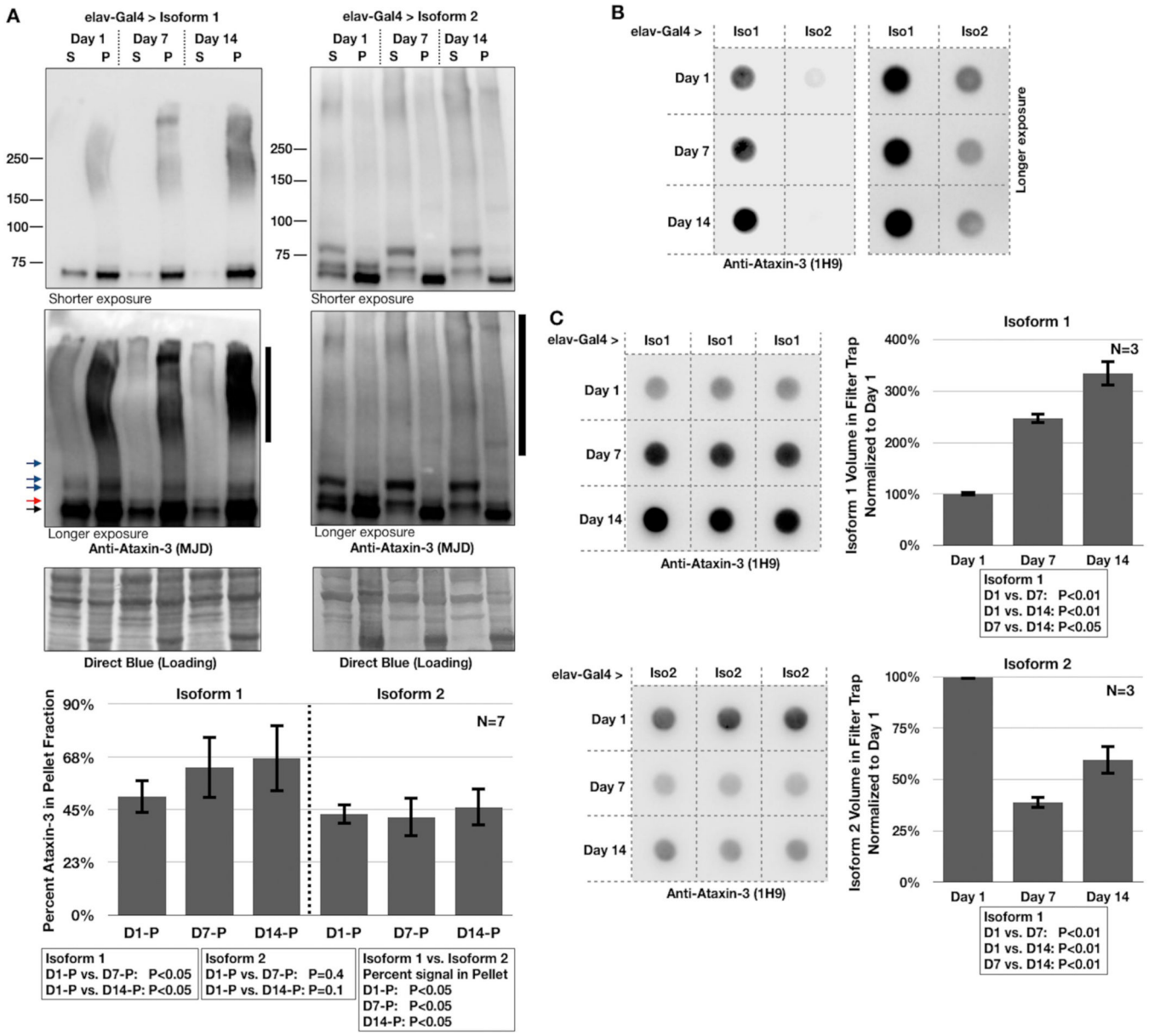

Fig. 5. Ataxin-3 isoform aggregation in fly neurons.

A) Western blots from adult flies expressing isoform 1 or 2 of pathogenic ataxin-3 in all neurons throughout development and in adults, harvested on the indicated days. Fly lysates were separated into soluble (S) and insoluble (P) fractions and loaded onto SDS-PAGE gels. Signal from the entire length of each isoform lane was quantified, normalized to loading control and expressed as percent ataxin-3 signal in the pellet fraction compared to the total signal. Black bars on the right side of longer exposure blots indicate SDS-resistant species whose migration over time shifts to higher molecular weight markers for isoform 1. Shown in histograms are means ± SD. *P* values from ANOVA with Tukey's post-hoc. Samples from isoforms 1 and 2 were loaded onto different gels to avoid the need for over-exposure of isoform 1 to visualize and quantify isoform 2. Black arrow: main ataxin-3 band. Red arrow: potentially phosphorylated form of ataxin-3. Blue arrows: ubiquitinated species of ataxin-3.

B) Filter-trap assay of flies expressing isoform 1 or 2 in neurons, harvested at the indicated days.

C) Independent filter-trap assays from isoforms 1 and 2 were loaded separately to avoid the need for over-exposure of isoform 1 to visualize and quantify isoform 2. Shown in histograms are means ± SD. *P* values from ANOVA with Tukey's post-hoc. For panels (B) and (C): Iso: isoform. (For interpretation of the references to colour in this figure legend, the reader is referred to the web version of this article.)

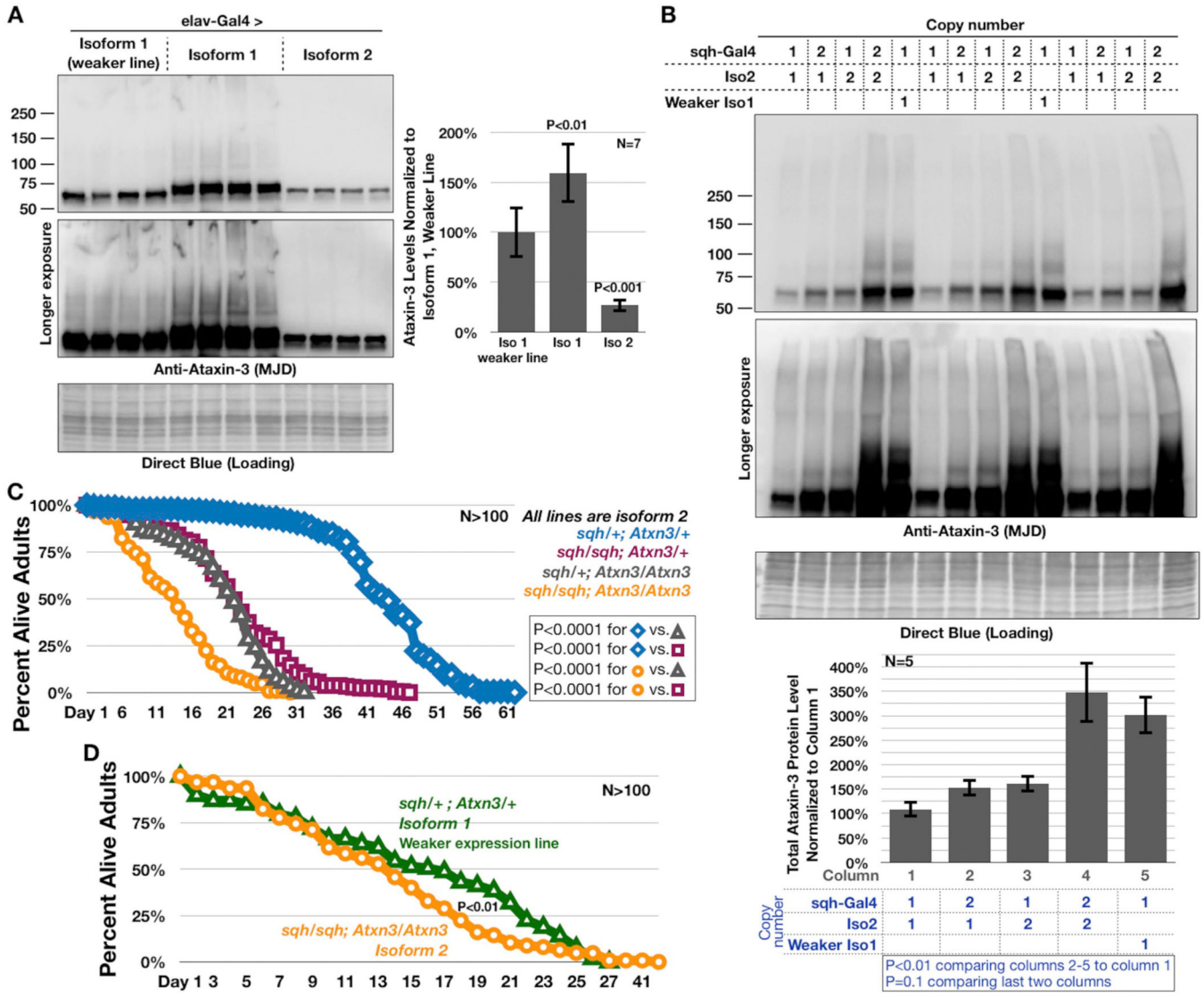

Fig. 6. Isoform 2 is no less toxic than isoform 1 when at comparable protein levels.

A) Western blots of flies expressing the noted ataxin-3 isoform transgenes in all neurons. Flies were one day old. Shown in histograms are means ± SD. *P* values from student's *t*-tests comparing isoform 1 and isoform 2 to the weaker isoform 1. For these blots we utilized the pan-neuronal Gal4 driver, since use of the ubiquitous one results in late pupal and pharate adult lethality from isoform 1. For a blot showing levels of the three ataxin-3 transgenes when expressed ubiquitously in flies, see Supplemental fig. 4 where we show results from pupal lysates.

B) Western blots of one-day-old adult flies with the noted genotypes. Each lane is an independent repeat. Shown in graph are means ± SD. *P* values from ANOVA with Tukey's post-hoc. Iso: isoform.

C) Longevity assays when flies express isoform 2 in all tissues. sqh-Gal4 was the driver. For perspective, flies without pathogenic ataxin-3 live > 70 days (*e.g.* Fig. 3). *P* values from log-rank tests.

D) Longevity of adult flies with the noted copies and transgenes. Curve from isoform 2 is the same as in panel C, since these assays were conducted at the same time. *P* value from log-rank test.

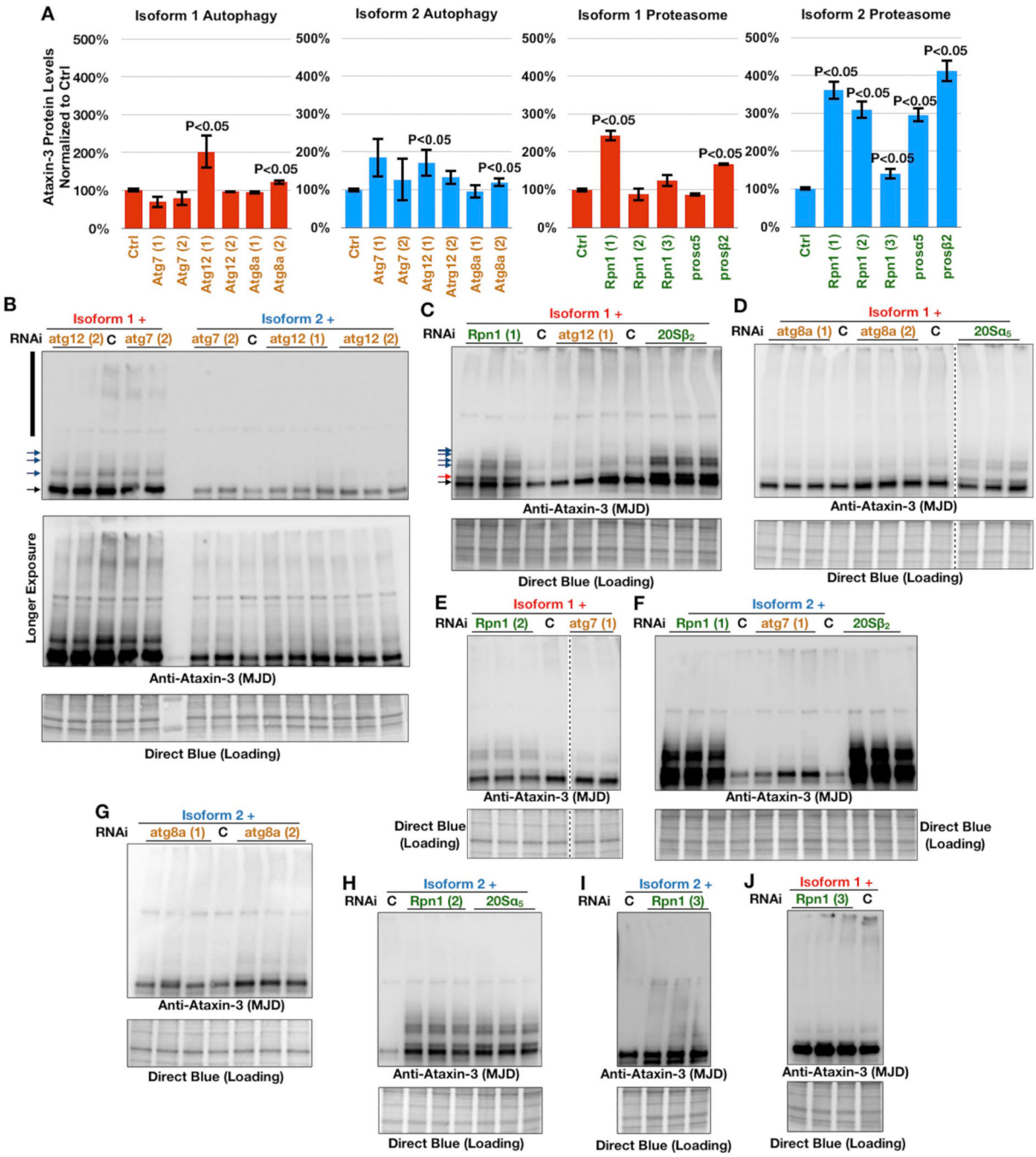

Fig. 7. Knockdown of autophagy or proteasome components leads to increased isoform protein levels in *Drosophila.*

A) Summary of quantification of the data in panels B-J and other experimental repeats not included. Histograms show means ± SD. *P* values from student's *t*-tests. $N \geq 3$ for each group.

B–J) Western blots of dissected fly heads expressing either isoform 1 or 2 of pathogenic ataxin-3 on RNAi control background or with RNAi constructs targeting the noted genes. Numbers associated with RNAi lines indicate different constructs targeting the same gene. Lack of numbers means that only one RNAi line was at hand for that gene. Black arrow:

main ataxin-3 band. Red arrow: potentially phosphorylated form of ataxin-3. Blue arrows: ubiquitinated species of ataxin-3. Black bar in panel (B): SDS-resistant species. In panels D and E, images are from the same membrane, same exposure, cropped and rearranged for viewing. C: controls, containing the driver (GMR-Gal4) and either isoform of ataxin-3 on the genetic background of the RNAi line. Signal was quantified from the entire lane for each well and used in panel (A). (For interpretation of the references to colour in this figure legend, the reader is referred to the web version of this article.)

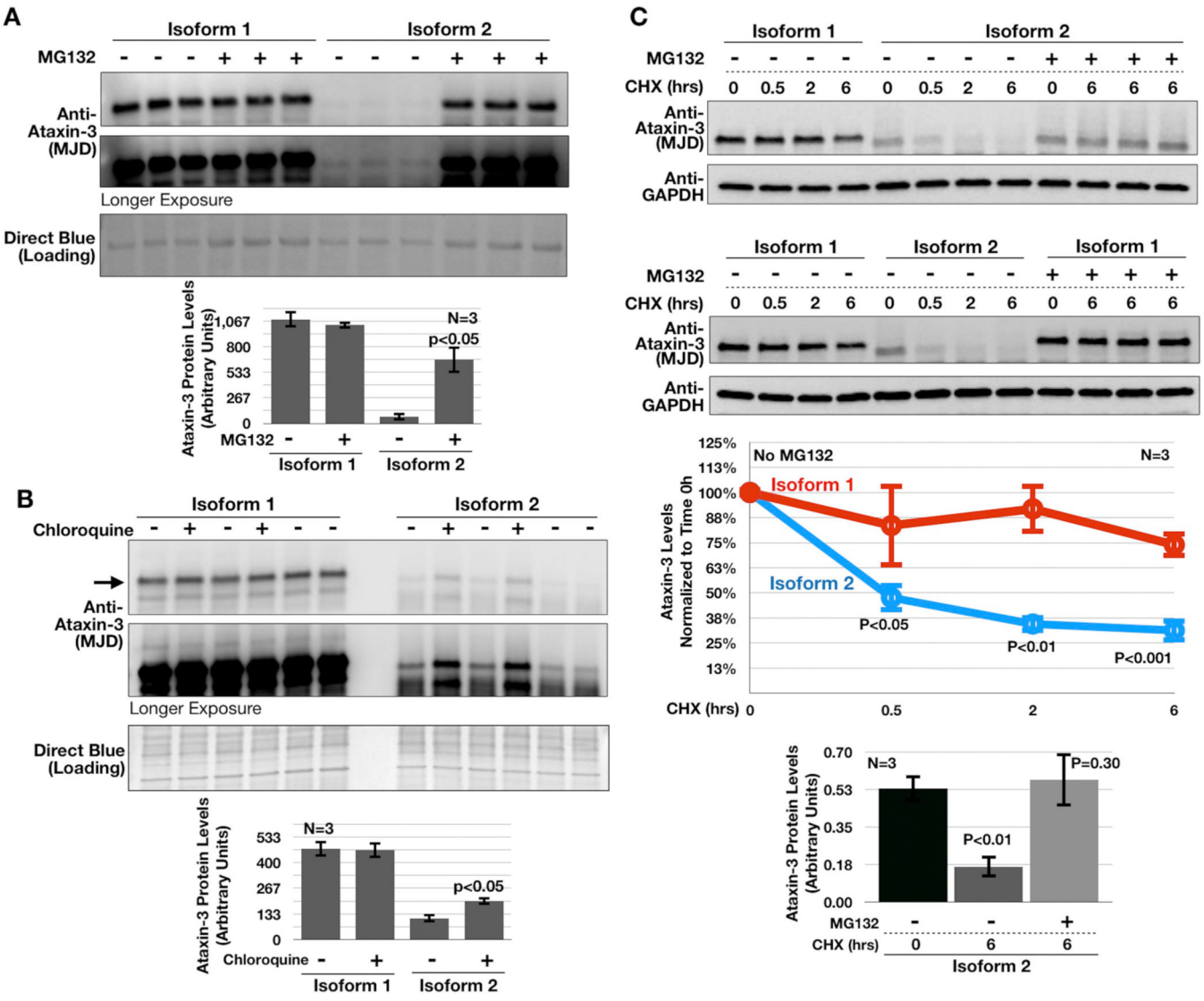

Fig. 8. Isoform 2 is turned over more rapidly in HeLa cells.

A & B) Western blots from HeLa cells transiently transfected with plasmids encoding either isoform of pathogenic ataxin-3 and treated, or not, with the proteasome inhibitor MG132 (20 μM) or with chloroquine (100 μM) for 6 h before harvesting. Every lane is from an independent repeat. Each well of cells received 1 μg plasmid of the indicated isoform. Arrow in (B): main ataxin-3 band. Histograms are from blots above and other independent repeats. *P* values from student's *t*-tests comparing treated lanes to respective untreated lanes of the same construct.

C) Western blots of whole cell lysates from HeLa cells transiently transfected as noted then treated with cycloheximide (CHX; 100 μg/ml) for the indicated amounts of time, as well as MG132, where applicable (20 μM). Wells received a higher amount of isoform 2 than isoform 1 (4:1 ratio; isoform 1 plasmid was supplemented with empty vector to bring it to the same total amount as isoform 2) to more closely approximate the amount of isoform 2 protein to isoform 1 at time 0 h. The two sets of blots are from independent experiments. Quantifications are from blots on the top and other, independent repeats. *P* values from

student's *t*-tests comparing isoform 2 to isoform 1 for the middle graph, and the two right columns to the left-most column in the bottom graph. Shown in graphs are means ± SD.

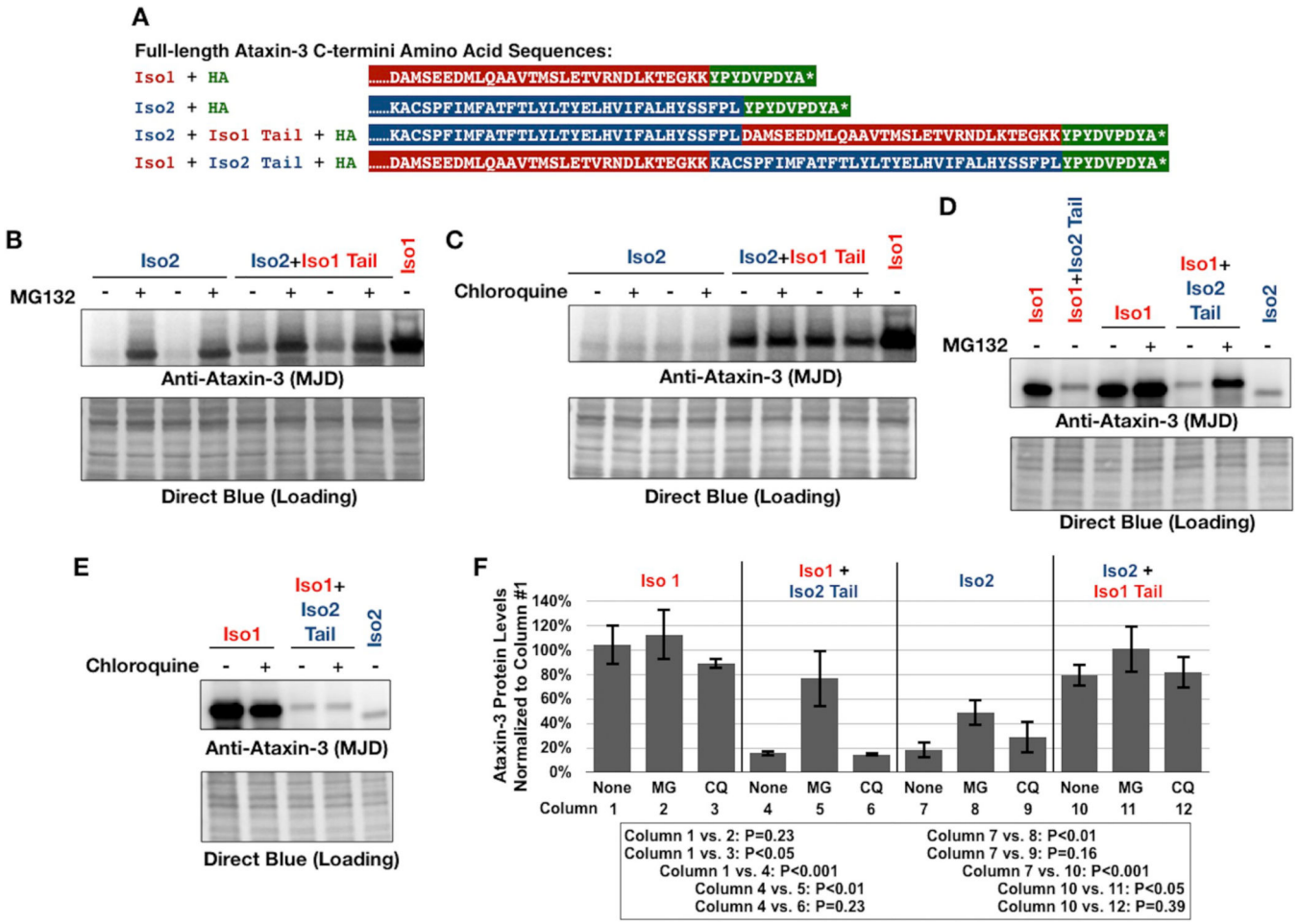

Fig. 9. The C-termini of isoforms 1 and 2 are important for host protein levels.

A) Summary of constructs generated and used in panels B–E.

B–E) Western blots of whole cell lysates from HEK-293T cells transiently transfected with 0.5 μg of the indicated plasmids and then treated, or not, for 6 h with MG132 (20 μM; panels B & D) or chloroquine (100 μM; panels C & E). Each lane is from an independent repeat.

F) Histograms from samples in panels B–E and other experimental repeats. N ≥ 3 for each group. *P* values from ANOVA with Tukey's post-hoc. For all panels, Iso: isoform. MG: MG132, CQ: Chloroquine.